

High Dimensional Semiparametric Gaussian Copula Graphical Models

Han Liu, Fang Han, Ming Yuan, John Lafferty and Larry Wasserman

February 9, 2012

Abstract: In this paper, we propose a semiparametric approach, named *nonparanormal* SKEPTIC, for efficiently and robustly estimating high dimensional undirected graphical models. To achieve modeling flexibility, we consider Gaussian Copula graphical models (or the nonparanormal) as proposed by Liu et al. (2009). To achieve estimation robustness, we exploit nonparametric rank-based correlation coefficient estimators, including Spearman’s rho and Kendall’s tau. In high dimensional settings, we prove that the nonparanormal SKEPTIC achieves the optimal parametric rate of convergence in both graph and parameter estimation. This celebrating result suggests that the Gaussian copula graphical models can be used as a safe replacement of the popular Gaussian graphical models, even when the data are truly Gaussian. Besides theoretical analysis, we also conduct thorough numerical simulations to compare different estimators for their graph recovery performance under both ideal and noisy settings. The proposed methods are then applied on a large-scale genomic dataset to illustrate their empirical usefulness. The R language software package **huge** implementing the proposed methods is available on the Comprehensive R Archive Network: <http://cran.r-project.org/>.

Keywords and phrases: high dimensional statistics, undirected graphical models, Gaussian copula, nonparanormal graphical models, robust statistics, minimax optimality, biological regulatory networks.

Contents

1	Introduction	2
2	Background	4
	2.1 The Nonparanormal	5
	2.2 The Normal-score based Nonparanormal Graph Estimator	6
3	The Nonparanormal SKEPTIC	9
	3.1 Main Idea	9
	3.2 The Nonparanormal SKEPTIC with Different Graph Estimators	10
	3.3 Computational Complexity	12
	3.4 Estimating Marginal Transformations	12
4	Theoretical Properties	13
	4.1 Concentration Properties of the Estimated Correlation Matrices	13
	4.2 Applying the Nonparanormal SKEPTIC with the graphical Dantzig Selector	14
5	Experimental Results	15

5.1	Summary of the Experimental Results	16
5.2	Numerical Simulations	16
5.3	Gene Expression Data	28
6	Conclusions	31
	Acknowledge	31
A	Proofs of Main Results	32
A.1	Proof of Proposition 3.1	32
A.2	Proof of Theorem 4.2	33
A.3	Proof of Theorem 4.1	33
B	Other Proofs	35
B.1	Some Useful Lemmas	35
B.2	Proof of Theorem 3.1	39
	References	40

1. Introduction

Undirected graphical models provide a powerful framework to explore the interrelationship among a large number of random variables, and have found routine use in analyzing complex and high dimensional data ranging from high throughput genomic experiments, functional Magnetic Resonance Imaging (fMRI), to mass spectrometry analysis.

An undirected graph $G = (V, E)$ consists of a set of vertices $V = \{1, \dots, d\}$ and a set of unordered pairs E representing edges between the vertices. Each vertex i corresponds to the random variable X_i . A joint distribution P for the random vector $X = (X_1, \dots, X_d)^T$ is Markov to $G = (V, E)$ if the following condition holds: X_i is independent of X_j given $(X_k : k \neq i, j)$ if and only if $(i, j) \notin E$. In a graph estimation problem, we have n observations of the random vector X , and want to estimate the edge set E .

The most common method for estimating E when the dimension d is small is to assume that Y has a multivariate Gaussian distribution with inverse covariance matrix (also called *concentration* matrix or *precision* matrix) Ω , then test the sparsity pattern of Ω (Dempster, 1972; Edwards, 1995). Drton and Perlman (2007, 2008) have developed this method in detail. A drawback is that the dimensionality d must be strictly smaller than n .

In high dimensional setting (when $d > n$), Meinshausen and Bühlmann (2006) proposed a pseudo-likelihood based approach to estimate graphs under Gaussian models. They use the lasso (Chen et al., 1998; Tibshirani, 1996) to regress X_i on $(X_j : j \neq i)$. This is repeated for each X_i . Let

$$\beta^i = \operatorname{argmin}_{\beta} \mathbb{E} \left(X_i - \sum_{j \neq i} \beta_j X_j \right)^2 \quad (1.1)$$

and define the neighborhood of i , $N_i := \{j : \beta_j^i \neq 0\}$. The lasso gives estimates $\hat{\beta}^i$ for all i . Let $\hat{N}_i := \{j : \hat{\beta}_j^i \neq 0\}$ and \hat{E} be the set of edges (i, j) such that $i \in \hat{N}_j$ and $j \in \hat{N}_i$. Under

suitable sparsity assumptions they prove that $\mathbb{P}(N_i = \hat{N}_i) \rightarrow 1$ as $n \rightarrow \infty$ even if $d = n^\gamma$ for some $\gamma > 0$. Similarly, $\mathbb{P}(E = \hat{E}) \rightarrow 1$ as $n \rightarrow \infty$. For discrete data, Ravikumar et al. (2010) proposed a similar pseudo-likelihood procedure for estimating high dimensional Ising models (or discrete Markov random fields). The main difference is that they replace the lasso with L_1 -regularized logistic regression.

Alternatively, Yuan and Lin (2007) proposed a penalized likelihood estimator

$$\hat{\Omega} = \arg \max_{\Omega \succeq 0} \{ \text{loglikelihood}(\Omega) - \lambda \sum_{j \neq k} |\Omega_{jk}| \} \quad (1.2)$$

where the loglikelihood of Ω is evaluated under the Gaussian model, with Ω as precision matrix. The estimator $\hat{\Omega}$ can be efficiently computed using the glasso algorithm (Banerjee et al., 2008; Friedman et al., 2008), which is a block coordinate descent procedure that uses the standard lasso to estimate a single row and column of Ω in each iteration. The resulting estimator $\hat{\Omega}$ has been shown to have good theoretical properties (Lam and Fan, 2009; Peng et al., 2009; Ravikumar et al., 2009; Rothman et al., 2008).

More recently it has been introduced a method named graphical Dantzig selector (or gDantzig), which estimates the precision matrix column by column using the Dantzig selector (Yuan, 2010). In terms of L_1 -risk, the graphical Dantzig selector is minimax optimal over certain model class. Another graph and precision matrix estimation method named CLIME is developed by Cai et al. (2011). The rate of convergence and optimality properties of the CLIME have also been established.

Despite the popularity of the Gaussian graphical model, its normality assumption is rather restrictive. If this parametric normality assumption is correct, accurate and precise estimates can be expected. However, given the increasing complexity of modern datasets, conclusions inferred under such a restrictive assumption could be misleading. In fact, besides high dimensionality, modern scientific datasets pose two additional challenges:

- **Challenge 1:** the distributions of the data are in general non-Gaussian;
- **Challenge 2:** the data could be noisy (e.g. contaminated by outliers).

To handle the first challenge, Liu et al. (2009) proposed the *nonparanormal*, which exploits the semiparametric Gaussian copula model to relax the Gaussian assumption. A random vector X belongs to a nonparanormal family if there exists a set of univariate monotone functions $\{f_j\}_{j=1}^d$ such that $f(X) := (f_1(X_1), \dots, f_d(X_d))^T$ is Gaussian. Liu et al. (2009) show that the nonparanormal family is equivalent to the Gaussian copula family (Klaassen and Wellner, 1997; Tsukahara, 2005), and provide a learning algorithm that has the same computational cost as the glasso. They first use a Winsorized estimator to estimate the marginal transformations f_j , then estimate the precision matrix using the transformed data. A rate of convergence $O(\sqrt{n^{-1/2} \log d})$ is established for estimating the precision matrix in terms of Frobenius and spectral norms. However, it is not clear whether their obtained rate of convergence is optimal or not.

In this paper we show that the rate of convergence obtained by Liu et al. (2009) is not optimal. We present an alternative procedure that simultaneously achieves estimation robustness and rate optimality. The main idea is to exploit robust nonparametric rank-based statistics including Spearman’s rho and Kendall’s tau to directly estimate the unknown correlation matrix, without explicitly calculating the marginal transformations. We call this approach the *nonparanormal* SKEPTIC (since the Spearman/Kendall estimates preempt transformations to inter correlation). The estimated correlation matrix is then plugged into existing parametric procedures (graphical lasso, CLIME, or graphical Dantzig selector) to obtain the final estimate of the inverse correlation matrix and the graph.

By leveraging existing analysis of different parametric methods (Cai et al., 2011; Lam and Fan, 2009; Ravikumar et al., 2009; Yuan, 2010), we prove that although the nonparanormal is a strictly larger family of distributions than the Gaussian, the nonparanormal SKEPTIC achieves the optimal parametric rate $O(\sqrt{n^{-1} \log d})$ in terms of precision matrix estimation. The extra modeling flexibility and robustness come at almost no cost of statistical efficiency. Thus this new estimator can be used as a safe replacement of Gaussian estimators even when the data are truly Gaussian. Moreover, by avoiding the estimation of the transformation functions, this new approach has fewer tuning parameters than the nonparanormal estimator proposed by Liu et al. (2009).

We provide careful numerical studies to support our theory. Our results show that, when the data contamination rate is low, the normal-score based nonparanormal estimator proposed by Liu et al. (2009) is slightly more efficient than the nonparanormal SKEPTIC. However, when the data contamination rate is higher, the nonparanormal SKEPTIC clearly outperforms the normal-score based nonparanormal estimator. This result reflects the tradeoff of statistical efficiency with estimation robustness.

This paper is organized as the following. In the next section we briefly review some background of the nonparanormal estimator from Liu et al. (2009). In Section 3 we present the nonparanormal SKEPTIC estimator, which exploits the Spearman’s rho and Kendall’s tau statistics to estimate the underlying correlation matrix. We present a theoretical analysis of the method in Section 4, with more detailed proofs collected in the appendix. In Section 5 we present numerical results on both simulated and real data, where the problem is to construct large undirected graphs for different biological entities (different tissue types or genes using very large-scale genomic datasets). We then discuss the connections to existing methods and possible future directions in the last section.

2. Background

In this section we briefly describe the nonparanormal family and the normal-score based graph estimator proposed by Liu et al. (2009).

Let $A = [A_{jk}] \in \mathbb{R}^{d \times d}$ and $v = (v_1, \dots, v_d)^T \in \mathbb{R}^d$. For $1 \leq q < \infty$, we define

$$\|v\|_q = \left(\sum_{i=1}^d |v_i|^q \right)^{1/q} \quad \text{and} \quad \|v\|_\infty = \max_{1 \leq i \leq d} |v_i|.$$

For $1 \leq q \leq \infty$, we define the matrix ℓ_q -operator norm:

$$\|A\|_q = \sup_{v \neq 0} \frac{\|Av\|_q}{\|v\|_q}.$$

For $q = 1$ and $q = \infty$, the matrix norm can be more explicitly represented as

$$\|A\|_1 = \max_{1 \leq j \leq d} \sum_{i=1}^d |A_{ij}| \quad \text{and} \quad \|A\|_\infty = \max_{1 \leq i \leq d} \sum_{j=1}^d |A_{ij}|.$$

The matrix ℓ_2 -operator norm is the leading singular value and is often called the spectral norm. We also define $\|A\|_{\max} = \max_{j,k} |A_{jk}|$ and $\|A\|_F^2 = \sum_{j,k} |A_{jk}|^2$. We denote

$$v_{\setminus j} = (v_1, \dots, v_{j-1}, v_{j+1}, \dots, v_d)^T \in \mathbb{R}^{d-1},$$

and similarly denote by $A_{\setminus i, \setminus j}$ the submatrix of A obtained by removing the i^{th} row and j^{th} column. We use $A_{i, \setminus j}$ to represent the i^{th} row of A with its j^{th} entry removed. The notation $\lambda_{\min}(A)$ and $\lambda_{\max}(A)$ are used for the smallest and largest singular values of A .

2.1. The Nonparanormal

The general form for a (strictly positive) probability density encoded by an undirected graph G can be written as

$$p(x) = \frac{1}{Z(f)} \exp \left(\sum_{C \in \text{Cliques}(G)} f_C(x_C) \right), \quad (2.1)$$

where the sum is over all cliques, or fully connected subsets of vertices of the graph. In general, this is what we mean by a *nonparametric graphical model*. It is the graphical model analogue of the general nonparametric regression. Model (2.1) has two main ingredients, the graph G and the functions $\{f_C\}$. However, without further assumptions, it is much too general to be practical. The main difficulty in working with such a model is the normalizing constant $Z(f)$, which cannot, in general, be efficiently computed or approximated.

The nonparanormal distribution can be viewed as a subclass of nonparametric graphical models with more restrictive constraints. As has been discussed in Liu et al. (2009), the nonparanormal approach parallels the ideas behind sparse additive models for regression. Specifically, we replace the random variable $X = (X_1, \dots, X_d)^T$ by the transformed random variable $f(X) = (f_1(X_1), \dots, f_d(X_d))^T$, and assume that $f(X)$ is multivariate Gaussian. This

results in a nonparametric extension of the Normal. The nonparanormal only depend on the univariate functions $\{f_j\}$ and the correlation matrix Σ^0 , all of which are to be estimated from data. While the resulting family of distributions is much richer than the standard parametric Normal (the paranormal), the independence relations among the variables are still encoded in the precision matrix $\Omega^0 = (\Sigma^0)^{-1}$, as we will show below.

Definition 2.1 (Nonparanormal). Let $f = (f_1, \dots, f_d)$ be a set of monotone univariate functions and $\Sigma^0 \in \mathbb{R}^{d \times d}$ be a positive-definite correlation matrix, with

$$\text{diag}(\Sigma^0) = \mathbf{1}. \quad (2.2)$$

We say a d -dimensional random variable $X = (X_1, \dots, X_d)^T$ has a nonparanormal distribution $X \sim \text{NPN}_d(f, \Sigma^0)$ if $f(X) := (f_1(X_1), \dots, f_d(X_d))^T \sim N(0, \Sigma^0)$.

For continuous distributions, Liu et al. (2009) proved that the nonparanormal family is equivalent to the Gaussian copula family (Klaassen and Wellner, 1997; Tsukahara, 2005). Figure 1 shows three examples of bivariate nonparanormal densities. The component functions are taken to be from three different families of monotonic functions—one using power transforms, one using logistic transforms, and another using sinusoids:

$$f_\alpha(x) = \text{sign}(x)|x|^\alpha \quad (2.3)$$

$$g_\alpha(x) = \lfloor x \rfloor + \frac{1}{1 + \exp\{-\alpha(x - \lfloor x \rfloor - \frac{1}{2})\}} \quad (2.4)$$

$$h_\alpha(x) = x + \frac{\sin(\alpha x)}{\alpha}. \quad (2.5)$$

The covariance in each case is $\Sigma = \begin{pmatrix} 1 & .5 \\ .5 & 1 \end{pmatrix}$ and the mean is $\mu = (0, 0)^T$. It can be seen how the concavity and number of modes of the density can change with different nonlinearities. Clearly the nonparanormal family is much richer than the Normal family.

Let $\Omega^0 = (\Sigma^0)^{-1}$ be the precision matrix. It has been proved that the sparsity pattern of Ω^0 encodes the undirected graph of X (Liu et al., 2009); that is,

$$\Omega_{jk}^0 = 0 \Leftrightarrow X_j \perp\!\!\!\perp X_k \mid X_{\setminus\{j,k\}}. \quad (2.6)$$

Therefore, even the nonparanormal family is larger than the Gaussian family, its conditional independence graph is encoded by the sparsity pattern of Ω^0 .

2.2. The Normal-score based Nonparanormal Graph Estimator

Liu et al. (2009) suggest a two-step procedure to estimate the graph.

1. Replace the observations, for each variable, by their respective Normal scores.
2. Apply the glasso to the transformed data to estimate the undirected graph.

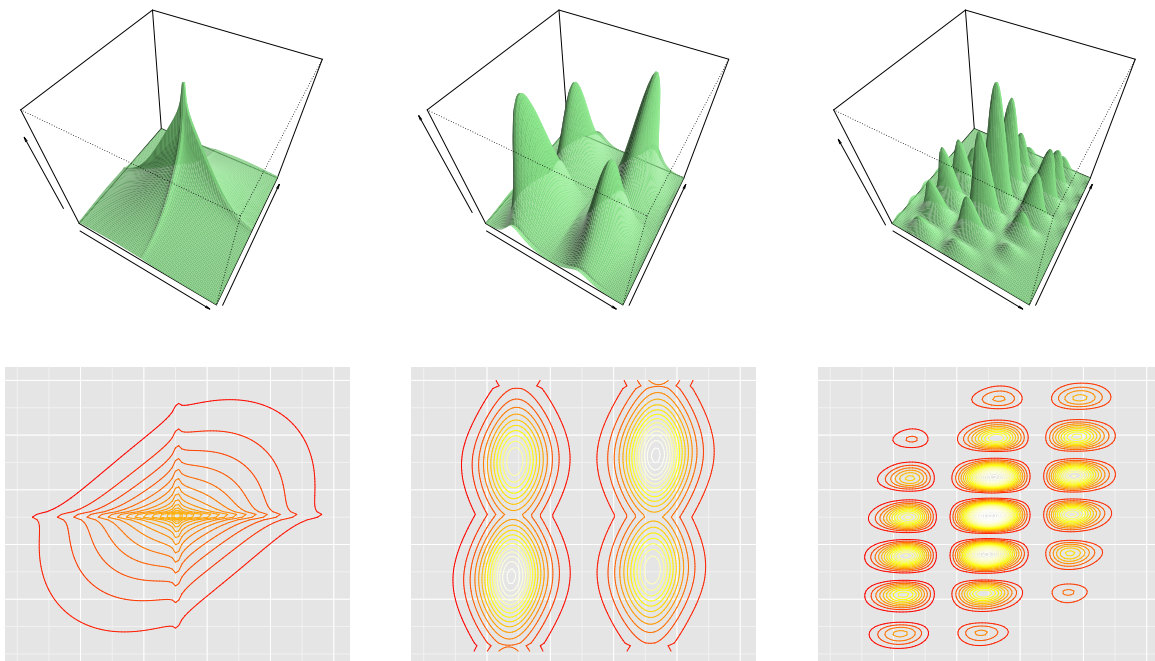


FIG 1. *Densities of three bivariate nonparanormals. The left plots have component functions of the form $f_\alpha(x) = \text{sign}(x)|x|^\alpha$, with $\alpha_1 = 0.9$, and $\alpha_2 = 0.8$. The center plots have component functions of the form $g_\alpha(x) = \lfloor x \rfloor + 1/(1 + \exp(-\alpha(x - \lfloor x \rfloor - 1/2)))$ with $\alpha_1 = 10$ and $\alpha_2 = 5$, where $x - \lfloor x \rfloor$ is the fractional part. The right plots have component functions of the form $h_\alpha(x) = x + \sin(\alpha x)/\alpha$, with $\alpha_1 = 5$ and $\alpha_2 = 10$. In each case $\mu = (0, 0)^T$ and $\Sigma = \begin{pmatrix} 1 & .5 \\ .5 & 1 \end{pmatrix}$.*

More specifically, let $x^1, \dots, x^n \in \mathbb{R}^d$ be n data points and let $I(\cdot)$ be the indicator function. We define

$$\hat{F}_j(t) = \frac{1}{n+1} \sum_{i=1}^n I(x_j^i \leq t) \quad (2.7)$$

to be the scaled empirical cumulative distribution function of X_j . Liu et al. (2009) study the estimates of the nonparanormal transformation functions given by¹

$$\hat{f}_j(t) = \Phi^{-1} \left(T_{\delta_n}[\hat{F}_j(t)] \right),$$

where T_{δ_n} is a Winsorization (or truncation) operator defined as

$$T_{\delta_n}(x) = \delta_n \cdot I(x < \delta_n) + x \cdot I(\delta_n \leq x \leq 1 - \delta_n) + (1 - \delta_n) \cdot I(x > 1 - \delta_n).$$

¹Instead of \hat{F}_j , Liu et al. (2009) use the empirical cumulative distribution function. These two estimators are asymptotically equivalent.

Let $\widehat{S}^{\text{ns}} = [\widehat{S}_{jk}^{\text{ns}}]$ be the correlation matrix of the transformed data, where

$$\widehat{S}_{jk}^{\text{ns}} = \frac{\frac{1}{n} \sum_{i=1}^n \widehat{f}_j(x_j^i) \widehat{f}_k(x_k^i)}{\sqrt{\frac{1}{n} \sum_{i=1}^n \widehat{f}_j^2(x_j^i)} \cdot \sqrt{\frac{1}{n} \sum_{i=1}^n \widehat{f}_k^2(x_k^i)}}. \quad (2.8)$$

The nonparanormal estimate of the inverse correlation matrix $\widehat{\Omega}^{\text{ns}}$ can be obtained by plugging \widehat{S}^{ns} into the glasso.

It is easy to see that if we take $\delta_n = \frac{1}{n+1}$, $\widehat{S}_{jk}^{\text{ns}}$ is called *the normal-score rank correlation coefficient*. For bivariate Gaussian copula distributions, Klaassen and Wellner (1997) have proved that $\widehat{S}_{jk}^{\text{ns}}$ is semi parametric efficient in estimating Σ_{jk}^0 . However, their efficiency result can not be straightforwardly generalized to high dimensions. The main reason is that the Gaussian quantile function $\Phi^{-1}(\cdot)$ diverges very quickly when evaluated at a point close to 1. To handle high dimensional cases, Liu et al. (2009) suggest a truncation level

$$\delta_n = \frac{1}{4n^{1/4} \sqrt{\pi \log n}}. \quad (2.9)$$

Such a truncation level δ_n is chosen to control the tradeoff the bias and variance in high dimensions. They analyze the high dimensional scaling of the precision matrix estimator $\widehat{\Omega}^{\text{ns}}$ and show that

$$\|\widehat{\Omega}^{\text{ns}} - \Omega^0\|_F = O_P \left(\sqrt{\frac{(s+d) \log d + \log^2 n}{n^{1/2}}} \right) \quad (2.10)$$

$$\|\widehat{\Omega}^{\text{ns}} - \Omega^0\|_2 = O_P \left(\sqrt{\frac{s \log d + \log^2 n}{n^{1/2}}} \right), \quad (2.11)$$

where $s := \text{Card}(\{(i, j) \in \{1, \dots, d\} \times \{1, \dots, d\} \mid \Omega_{jk}^0 \neq 0, i \neq j\})$ is the number of nonzero off-diagonal elements of the true precision matrix.

Using the results of Ravikumar et al. (2009), it can also be shown that, under appropriate conditions, the sparsity pattern of the precision matrix can be accurately recovered with high probability. In particular, the nonparanormal estimator $\widehat{\Omega}^{\text{ns}}$ satisfies

$$\mathbb{P} \left(\mathcal{G} \left(\widehat{\Omega}^{\text{ns}}, \Omega^0 \right) \right) \geq 1 - o(1)$$

where $\mathcal{G}(\widehat{\Omega}^{\text{ns}}, \Omega^0)$ is the event $\left\{ \text{sign} \left(\widehat{\Omega}_{jk}^{\text{ns}} \right) = \text{sign} \left(\Omega_{jk}^0 \right), \forall j, k \in \{1, \dots, d\} \right\}$. We refer to Liu et al. (2009) for more details of the technical conditions and proofs.

As has been discussed by Liu et al. (2009), it is not clear whether the obtained rates in (2.10) and (2.11) are optimal or not. In this paper, we show that these rates are not optimal and can be greatly improved using different estimators.

3. The Nonparanormal SKEPTIC

In this section we propose a different approach for estimating Ω^0 that achieves a much faster rate of convergence, without explicitly estimating the transformation functions.

3.1. Main Idea

The main idea behind our alternative procedure is to exploit the Spearman's rho and Kendall's tau statistics to directly estimate the unknown correlation matrix, without explicitly calculating the marginal transformation functions f_j .

Let r_j^i be the rank of x_j^i among x_j^1, \dots, x_j^n and $\bar{r}_j = \frac{1}{n} \sum_{i=1}^n r_j^i$. We consider the following statistics:

$$\text{(Spearman's rho)} \quad \hat{\rho}_{jk} = \frac{\sum_{i=1}^n (r_j^i - \bar{r}_j)(r_k^i - \bar{r}_k)}{\sqrt{\sum_{i=1}^n (r_j^i - \bar{r}_j)^2 \cdot \sum_{i=1}^n (r_k^i - \bar{r}_k)^2}}, \quad (3.1)$$

$$\text{(Kendall's tau)} \quad \hat{\tau}_{jk} = \frac{2}{n(n-1)} \sum_{1 \leq i < i' \leq n} \text{sign}(x_j^i - x_j^{i'}) (x_k^i - x_k^{i'}). \quad (3.2)$$

Both can be viewed as a form of nonparametric correlation between the empirical realizations of two random variables X_j and X_k . Note that these statistics are invariant under monotone transformations. For Gaussian random variables there is a one-to-one mapping between these two statistics; details can be found in Kruskal (1958). Let \tilde{X}_j and \tilde{X}_k be two independent copies of X_j and X_k . We denote by F_j and F_k the CDFs of X_j and X_k . The population versions of Spearman's rho and Kendall's tau are given by

$$\rho_{jk} := \text{Corr}(F_j(X_j), F_k(X_k)), \quad (3.3)$$

$$\tau_{jk} := \text{Corr}(\text{sign}(X_j - \tilde{X}_j), \text{sign}(X_k - \tilde{X}_k)). \quad (3.4)$$

Both ρ_{jk} and τ_{jk} are association measures based on the notion of concordance. We call two pairs of real numbers (s, t) and (u, v) concordant if $(s - t)(u - v) > 0$ and discordant if $(s - t)(u - v) < 0$. The following proposition provides further insight into the relationship between ρ_{jk} and τ_{jk} . The proof is provided in the appendix for completeness.

Proposition 3.1. *Let $(X_j^{(1)}, X_k^{(1)})$, $(X_j^{(2)}, X_k^{(2)})$, and $(X_j^{(3)}, X_k^{(3)})$ be three independent random vectors with the same distribution as (X_j, X_k) . Define*

$$\begin{aligned} \mathcal{C}(j, s, t; k, u, v) &= \mathbb{P}((X_j^{(s)} - X_j^{(t)})(X_k^{(u)} - X_k^{(v)}) > 0), \\ \mathcal{D}(j, s, t; k, u, v) &= \mathbb{P}((X_j^{(s)} - X_j^{(t)})(X_k^{(u)} - X_k^{(v)}) < 0). \end{aligned}$$

Then $\rho_{jk} = 3\mathcal{C}(j, 1, 2; k, 1, 3) - 3\mathcal{D}(j, 1, 2; k, 1, 3)$ and $\tau_{jk} = \mathcal{C}(j, 1, 2; k, 1, 2) - \mathcal{D}(j, 1, 2; k, 1, 2)$.

For Gaussian copula distributions, the following important lemma connects the Spearman's rho and Kendall's tau to the underlying Pearson correlation coefficient Σ_{jk}^0 .

Lemma 3.1 (Fang et al. (2002); Kruskal (1958)). *Assuming $X \sim NPN(f, \Sigma^0)$, we have*

$$\Sigma_{jk}^0 = 2 \sin\left(\frac{\pi}{6} \rho_{jk}\right) = \sin\left(\frac{\pi}{2} \tau_{jk}\right). \quad (3.5)$$

Motivated by this lemma, we define the following estimators $\hat{S}^\rho = [\hat{S}_{jk}^\rho]$ and $\hat{S}^\tau = [\hat{S}_{jk}^\tau]$ for the unknown correlation matrix Σ^0 :

$$\hat{S}_{jk}^\rho = \begin{cases} 2 \sin\left(\frac{\pi}{6} \hat{\rho}_{jk}\right) & j \neq k \\ 1 & j = k \end{cases} \quad \text{and} \quad \hat{S}_{jk}^\tau = \begin{cases} \sin\left(\frac{\pi}{2} \hat{\tau}_{jk}\right) & j \neq k \\ 1 & j = k \end{cases}. \quad (3.6)$$

As will be shown in later sections, the final graph estimators based on the Spearman's rho and Kendall's tau statistics have similar theoretical performance. In the following sections we omit the superscript ρ and τ and simply denote the estimated correlation matrix as \hat{S} .

3.2. The Nonparanormal SKEPTIC with Different Graph Estimators

The estimated correlation matrices \hat{S}^τ and \hat{S}^ρ can be directly plugged into different parametric Gaussian graph estimators to obtain the final precision matrix and graph estimates.

3.2.1. The Nonparanormal SKEPTIC with the Graphical Dantzig Selector

The main idea of the graphical Dantzig selector (Yuan, 2010) is to take advantage of the connection between multivariate linear regression and entries of the inverse covariance matrix. The detailed algorithm is listed in the following, where δ is the tuning parameter.

- Estimation: For $j = 1, \dots, d$, calculate

$$\hat{\theta}^j = \arg \min_{\theta \in \mathbb{R}^{d-1}} \|\theta\|_1 \text{ s.t. } \|\hat{S}_{\setminus j, j} - \hat{S}_{\setminus j, \setminus j} \theta\|_\infty \leq \delta, \quad (3.7)$$

$$\hat{\Omega}_{jj} = \left[1 - 2 \left(\hat{\theta}^j \right)^T \hat{S}_{\setminus j, j} + \left(\hat{\theta}^j \right)^T \hat{S}_{\setminus j, \setminus j} \hat{\theta}^j \right], \quad (3.8)$$

$$\text{and } \hat{\Omega}_{\setminus j, j} = -\hat{\Omega}_{jj} \hat{\theta}^j. \quad (3.9)$$

- Symmetrization:

$$\hat{\Omega} = \arg \min_{\Omega = \Omega^T} \|\Omega - \hat{\Omega}\|_1. \quad (3.10)$$

The algorithm iterates over all the dimensions. For the j^{th} dimension, we regress X_j on $X_{\setminus j}$ using the Dantzig selector. The obtained regression coefficients $\hat{\theta}_j$ can then be exploited to estimate the elements Ω_{jj}^0 and $\Omega_{\setminus j, j}^0$ in the inverse correlation matrix Ω^0 .

Within each iteration, the Dantzig selector selector in (3.7) can be formulated as a linear program. A more sophisticated path algorithm (DASSO) to solve the Dantzig selector has been developed by James et al. (2009).

3.2.2. The Nonparanormal SKEPTIC with the CLIME

The estimated correlation coefficient matrix \widehat{S} can also be plugged into the CLIME estimator (Cai et al., 2011), which is defined by

$$\widehat{\Omega} = \arg \min_{\Omega} \sum_{j,k} |\Omega_{jk}| \text{ s.t. } \|\widehat{S}\Omega - \mathbf{I}_d\|_{\max} \leq \Delta, \quad (3.11)$$

where Δ is the tuning parameter. Cai et al. (2011) show that this convex optimization can be decomposed into d vector minimization problems, each of which can be cast as a linear program. Thus the CLIME thus has the potential to scale to very large problems.

3.2.3. The Nonparanormal SKEPTIC with the Graphical Lasso

We could also plug in the estimated correlation coefficient matrix \widehat{S} into the graphical lasso:

$$\widehat{\Omega} = \arg \min_{\Omega \succeq 0} \left\{ \text{tr}(\widehat{S}\Omega) - \log |\Omega| + \lambda \sum_{j \neq k} |\Omega_{jk}| \right\}. \quad (3.12)$$

One thing to note is that \widehat{S} may not be positive semidefinite. Even though the formulation (3.12) is still convex, certain algorithms (like the blockwise-coordinate descent algorithm (Friedman et al., 2008)) may fail. However other algorithms like two-metric projected Newton method or first-order projection do not have such positive semidefiniteness assumptions. Since the graphical Dantzig selector and the CLIME can both be formulated as linear programs, they do require positive semidefiniteness of the input correlation matrix either.

Remark 3.1. The nonparanormal SKEPTIC can also be applied with the Meinshausen-Bühlmann procedure to estimate the graph. As has been discussed in (Friedman et al., 2008), the correlation matrix is also a sufficient statistic for the Meinshausen-Bühlmann procedure. However, in this case, we need to make sure that \widehat{S} is positive semidefinite. Otherwise, the algorithm may not converge. In our case, we first project \widehat{S} into the cone of positive semidefinite matrices. In particular, we need to solve the following convex optimization problem:

$$\widetilde{S} = \arg \min_{S \succeq 0} \|\widehat{S} - S\|_{\max}. \quad (3.13)$$

Here we use the sup-norm $\|\cdot\|_{\max}$ instead of the Hilbert-norm $\|\cdot\|_F$, due to theoretical concerns developed in the next section. It is easy to show that the optimization in (3.13) can be formulated as the dual of a graphical lasso problem with the smallest possible tuning parameter that still guarantees a feasible solution. Empirically, we can use a surrogate projection procedure that computes a singular value decomposition of \widehat{S} and truncates all of the negative singular values to be zero. We found that this procedure works well.

3.3. Computational Complexity

Compared to the corresponding parametric methods like the graphical lasso, graphical Dantzig selector, or CLIME, the only extra cost of the the nonparanormal SKEPTIC is the computation of \widehat{S} , which requires us to calculate $d(d-1)/2$ pairwise Spearman's rho or Kendal's tau statistics. A naive implementation of the Kendal's tau matrix requires $O(d^2n^2)$ computation. However, efficient algorithm based on sorting and balanced binary trees has been developed to calculate Kendal's tau statistic with a computational complexity $O(d^2n \log n)$. Details can be found in Christensen (2005).

If we assume that each data point is unique (no "ties" in computing ranks), then Spearman's rho statistic can be written as

$$\widehat{\rho}_{jk} = 1 - \frac{6}{n(n^2 - 1)} \sum_{i=1}^n (r_j^i - r_k^i)^2, \quad (3.14)$$

where r_j^i is the rank of x_j^i among x_j^1, \dots, x_j^n . Therefore, once the ranks are obtained, the statistic can be computed very efficiently. Calculating \widehat{S}^ρ has the cost $O(d^2n \log n)$.

3.4. Estimating Marginal Transformations

We could estimate the marginal transformation f_j using the following estimator:

$$\widehat{f}_j(x) := \Phi^{-1} \left(\widetilde{F}_j(x) \right).$$

where $\widetilde{F}_j(t)$ is defined as

$$\begin{aligned} \widetilde{F}_j(t) = & \frac{1}{n} \sum_{i=1}^n I(x_j^i \leq t) \cdot I \left(\frac{1}{2n} \leq t \leq 1 - \frac{1}{2n} \right) \\ & + \frac{1}{2n} \cdot I(t < \frac{1}{2n}) + \left(1 - \frac{1}{2n} \right) \cdot I \left(t > 1 - \frac{1}{2n} \right). \end{aligned} \quad (3.15)$$

It's easy to see that for any fixed t , $\widehat{f}_j(t)$ converges in probability to $f_j(t)$ pointwise with a parametric rate. Theorem 3.1 provides a stronger result that \widehat{f}_j converges to f_j uniformly over an expanding interval with high probability. The proof is provided in Appendix B.

Theorem 3.1. *Let $g_j := f_j^{-1}$ be the inverse function of f_j . For any $0 < \gamma < 7/4$, we define*

$$I_n := \left[g_j \left(-\sqrt{\left(\frac{7}{4} - \gamma \right) \log n} \right), g_j \left(\sqrt{\left(\frac{7}{4} - \gamma \right) \log n} \right) \right], \quad (3.16)$$

then $\sup_{t \in I_n} |\widehat{f}_j(t) - f_j(t)| = o_P(1)$.

4. Theoretical Properties

We analyze the statistical properties of the nonparanormal SKEPTIC estimator. Our main result shows that \widehat{S}^ρ and \widehat{S}^τ estimate the true correlation matrix Σ^0 in the optimal parametric rate in high dimensions. Such a result allows us to easily leverage existing analysis of different parametric methods (e.g. graphical lasso, graphical Dantzig, and CLIME) to analyze the nonparanormal SKEPTIC estimator.

Our main result, Theorem 4.3, provides a general statement that the nonparanormal SKEPTIC achieves the same graph recovery and parameter estimation performance as the corresponding parametric methods. Since the nonparanormal family is much richer than the Gaussian family, such a result suggests that the nonparanormal SKEPTIC could be a safe replacement of the Gaussian graphical models. We then use the graphical Dantzig selector as an example to illustrate this result. Similar analysis can be carried on for both the CLIME and graphical lasso. To simplify analysis, we assume that there are no ties in the ranks assigned to data points.

4.1. Concentration Properties of the Estimated Correlation Matrices

We first prove the concentration properties of the estimators \widehat{S}^ρ and \widehat{S}^τ . Let Σ_{jk}^0 be the Pearson's correlation coefficient between $f_j(X_j)$ and $f_k(X_k)$. In terms of $\|\cdot\|_{\max}$ norm, we show that both \widehat{S}^ρ and \widehat{S}^τ are close to Σ^0 with the optimal parametric rate. Our results are based on different versions of the Hoeffding's inequalities for U-statistics.

Theorem 4.1. *For any $0 < \alpha < 1$, whenever*

$$n \geq \max \left\{ \frac{1}{6 \log d} \left(\frac{\alpha}{1 - \alpha} \right)^2, \frac{\alpha \sqrt{6}}{3} \cdot \sqrt{\frac{n}{\log d}} + 2 \right\}, \quad (4.1)$$

we have

$$\mathbb{P} \left(\sup_{jk} \left| \widehat{S}_{jk}^\rho - \Sigma_{jk}^0 \right| > \frac{3\pi\sqrt{6}}{\alpha} \sqrt{\frac{\log d}{n}} \right) \leq \frac{2}{d^2}. \quad (4.2)$$

Therefore, let $\alpha = \frac{3\sqrt{6}}{8}$, then with probability at least $1 - d^{-2}$, for $n \geq \frac{21}{\log d} + 2$, we have

$$\sup_{jk} \left| \widehat{S}_{jk}^\rho - \Sigma_{jk}^0 \right| \leq 8\pi \sqrt{\frac{\log d}{n}}. \quad (4.3)$$

The next theorem illustrates the concentration property of \widehat{S}^τ .

Theorem 4.2. *For any $n > 1$, with probability at least $1 - 1/d$, we have*

$$\sup_{jk} \left| \widehat{S}_{jk}^\tau - \Sigma_{jk}^0 \right| \leq 2.45\pi \sqrt{\frac{\log d}{n}}. \quad (4.4)$$

With the above results we could easily build the following “meta” theorem, which shows that even though the nonparanormal SKEPTIC is a semiparametric estimator, it achieves the optimal parametric rate in high dimensions.

Theorem 4.3 (Main Theorem). *If we plug the estimated correlation matrix \widehat{S}^ρ or \widehat{S}^τ into the parametric graphical lasso (or the graphical Dantzig selector, or the CLIME). Under the same conditions on Σ^0 that ensure the consistency of these parametric methods, the nonparanormal SKEPTIC achieves the same **parametric rates of convergence** for both precision matrix estimation and graph recovery.*

Proof. The proof is based on the key observation that the sample correlation matrix \widehat{S} is a sufficient statistic for all three methods: the graphical lasso, graphical Dantzig selector, and CLIME. By examining their analysis as in (Cai et al., 2011; Ravikumar et al., 2009; Yuan, 2010), the sufficient condition of \widehat{S} to enable their analysis is that, there exists some constant c , such that

$$\mathbb{P} \left(\|\widehat{S} - \Sigma^0\|_{\max} > c \sqrt{\frac{\log d}{n}} \right) \leq 1 - \frac{1}{d}. \quad (4.5)$$

Which can be directly replaced by (4.3) and (4.4) from theorems 4.1 and 4.2. \square

Since the graphical lasso, graphical Dantzig selector, and the CLIME have been proved to be minimax optimal over certain parameter classes under the Gaussian model. Using the fact that the nonparanormal family is strictly larger than the Gaussian family. We could immediately justify the minimax optimality property of the nonparanormal estimator:

Corollary 4.1. *Over all the parameter spaces of Σ^0 such that the graphical lasso, graphical Dantzig, or CLIME are minimax optimal under Gaussian models, the corresponding nonparanormal SKEPTIC estimator is also minimax optimal for the same parameter space of Σ^0 under the nonparanormal model (or Gaussian copula model).*

The key message conveyed by the main theorem and the above corollary is that, in terms of statistical rates of convergence, the nonparanormal SKEPTIC can be a safe replacement of the Gaussian graphical models. The extra flexibility and robustness come at almost no cost (the same rate, but with a slightly relaxed constant). In the next subsection, we showcase the main theorem on the graphical Dantzig selector.

Remark 4.1. Even though in this section we only present the results on the graphical Dantzig selector, graphical lasso, and CLIME, similar arguments should hold for almost all methods that use the correlation matrix Σ^0 as a sufficient statistics.

4.2. Applying the Nonparanormal SKEPTIC with the graphical Dantzig Selector

In Theorem 4.3 we have shown that the nonparanormal SKEPTIC estimator \widehat{S} can be plugged into any parametric graph estimator and achieves the optimal parametric rate of convergence.

In this subsection we only use the graphical Dantzig selector as a show case to see how this main theorem can be detailized in specific applications.

We denote $\widehat{\Omega}^{\text{npn-s}}$ to be the inverse correlation matrix estimated by using the nonparametric SKEPTIC with the graphical Dantzig selector in (3.10). Given a matrix Ω , we define $\deg(\Omega) = \max_{1 \leq i \leq d} \sum_{j=1}^d I(|\Omega_{ij}| \neq 0)$. Following Yuan (2010), we consider a class of inverse correlation matrices defined by

$$\mathcal{M}_1(\kappa, \tau, M) := \left\{ \Omega : \Omega \succ \mathbf{0}, \text{diag}(\Omega^{-1}) = \mathbf{1}, \|\Omega\|_1 \leq \kappa, \right. \\ \left. \frac{1}{\tau} \leq \lambda_{\min}(\Omega) \leq \lambda_{\max}(\Omega) \leq \tau, \deg(\Omega) < M \right\},$$

where $\kappa, \tau > 1$. We then have the following corollary of Theorem 4.3.

Theorem 4.4. *For $1 \leq q \leq \infty$, there exists a constant C_1 that depends on $\kappa, \tau, \lambda_{\min}(\Omega^0)$, and $\lambda_{\max}(\Omega^0)$, such that*

$$\sup_{\Omega^0 \in \mathcal{M}_1(\kappa, \tau, M)} \|\widehat{\Omega}^{\text{npn-s}} - \Omega^0\|_q = O_P \left(M \sqrt{\frac{\log d}{n}} \right), \quad (4.6)$$

provided that $\lim_{n \rightarrow \infty} \frac{n}{M^2 \log d} = \infty$ and $\delta = C_1 \sqrt{\frac{\log d}{n}}$, for sufficiently large C_1 . Here δ is the tuning parameter used in (3.7).

Proof. The proof can be directly obtained by replacing Lemma 12 in Yuan (2010) with the result of Theorem 4.3. \square

The next theorem establishes the minimax lower bound for inverse correlation matrix estimation over the class $\mathcal{M}_1(\kappa, \tau, M)$.

Theorem 4.5 (Yuan (2010)). *Let $M (\log d/n)^{1/2} = o(1)$. Then there exists a constant $C > 0$ depending only on κ and τ such that*

$$\liminf_{n \rightarrow \infty} \inf_{\widehat{\Omega}} \sup_{\Omega^0 \in \mathcal{M}_1(\kappa, \tau, M)} \mathbb{P} \left(\|\widehat{\Omega} - \Omega^0\|_1 \geq CM \sqrt{\frac{\log d}{n}} \right) > 0,$$

where the infimum is taken over all estimates of Ω based on the observed data x^1, \dots, x^n .

From the above theorems, we see that the nonparametric SKEPTIC estimate of the inverse correlation matrix can achieve the parametric rate and is in fact minimax rate optimal over the parameter space $\mathcal{M}_1(\kappa, \tau, M)$ in terms of L_1 -risk.

5. Experimental Results

In this section we investigate the empirical performance of different graph estimation methods on both synthetic and real datasets. In particular we consider the following methods:

- **npn** – the original nonparanormal estimator from Liu et al. (2009).
- **normal** – the Gaussian graphical model (which relies on the Gaussian assumption).
- **npn-spearman** – the nonparanormal SKEPTIC using the Spearman’s rho.
- **npn-tau** – the nonparanormal SKEPTIC using the Kendall’s tau.
- **npn-ns** – the normal-score based estimator as in (2.8) with $\delta_n = \frac{1}{n+1}$.

5.1. Summary of the Experimental Results

To compare the graph estimation performance of the two procedures A and B , in the following we use $A >_{\text{slightly}} B$ to represent that A slightly outperforms B ; $A > B$ means A is better than B ; $A \gg B$ means A is significantly better than B ; while $A \approx B$ means A and B have similar performance.

Our main conclusions are listed as below:

- non-Gaussian data without outlier: $\text{npn-ns} \approx \text{npn} \approx \text{npn-spearman} \approx \text{npn-tau} \gg \text{normal}$.
- non-Gaussian data with low level of outlier: $\text{npn-tau} \approx \text{npn-spearman} > \text{npn} > \text{npn-ns} \gg \text{normal}$.
- non-Gaussian data with higher level of outlier: $\text{npn-tau} > \text{npn-spearman} \gg \text{npn} > \text{npn-ns} \gg \text{normal}$.
- Gaussian data with no outlier: $\text{normal} \approx \text{npn-ns} \approx \text{npn} >_{\text{slightly}} \text{npn-spearman} \approx \text{npn-tau}$.
- Gaussian data with low outlier: $\text{npn-tau} \approx \text{npn-spearman} > \text{npn} > \text{npn-ns} \gg \text{normal}$.
- Gaussian data with higher outlier: $\text{npn-tau} > \text{npn-spearman} > \text{npn} > \text{npn-ns} > \text{normal}$.

The above results illustrate a tradeoff of estimation robustness and statistical efficiency. For nonparanormal data without outlier, the **npn-ns** and **npn** behave similarly as the **npn-tau** and **npn-spearman**. However, if the data are contaminated by outliers, the **npn-tau** and **npn-spearman** outperform **npn-ns** and **npn** even when the contamination level is low. Overall, our practice shows that both the **npn-tau** and **npn-spearman** have a good balance of statistical efficiency and robustness.

Besides numerical simulations, we apply our method on a large-scale genomic dataset as an empirical case study. The implementations of these methods can be found in our R package named **huge**, which is freely available from CRAN.

5.2. Numerical Simulations

We adopt the same data generating procedure as in Liu et al. (2009). To generate a d -dimensional sparse graph $G = (V, E)$, let $V = \{1, \dots, d\}$ correspond to variables $X = (X_1, \dots, X_d)$. We associate each index $j \in \{1, \dots, d\}$ with a bivariate data point $(Y_j^{(1)}, Y_j^{(2)}) \in [0, 1]^2$ where

$$Y_1^{(k)}, \dots, Y_n^{(k)} \sim \text{Uniform}[0, 1]$$

for $k = 1, 2$. Each pair of vertices (i, j) is included in the edge set E with probability

$$\mathbb{P}\left((i, j) \in E\right) = \frac{1}{\sqrt{2\pi}} \exp\left(-\frac{\|y_i - y_j\|_n^2}{2s}\right) \quad (5.1)$$

where $y_i := (y_i^{(1)}, y_i^{(2)})$ is the empirical observation of $(Y_i^{(1)}, Y_i^{(2)})$ and $\|\cdot\|_n$ represents the Euclidean distance. Here, $s = 0.125$ is a parameter that controls the sparsity level of the generated graph. We restrict the maximum degree of the graph to be 4 and build the inverse correlation matrix Ω^0 according to $\Omega_{jk}^0 = 1$ if $j = k$, $\Omega_{jk}^0 = 0.245$ if $(j, k) \in E$, and $\Omega_{jk}^0 = 0$ otherwise. Here the value 0.245 guarantees positive definiteness of Ω^0 . Let $\Sigma^0 = (\Omega^0)^{-1}$. To obtain the correlation matrix, we simply rescale Σ^0 so that all its diagonal elements are 1. We then sample n data points x^1, \dots, x^n from the nonparanormal distribution $NPN_d(f^0, \Sigma^0)$ where for simplicity we use the same univariate transformations on each dimension, i.e., $f_1^0 = \dots = f_d^0 = f^0$. To sample data from the nonparanormal distribution, we also need $g^0 := (f^0)^{-1}$. The following two different transformations g^0 are used in the simulation:

Definition 5.1. (Gaussian CDF Transformation) Let g_0 be a univariate Gaussian cumulative distribution function with mean μ_{g_0} and the standard deviation σ_{g_0} :

$$g_0(t) := \Phi\left(\frac{t - \mu_{g_0}}{\sigma_{g_0}}\right).$$

The Gaussian CDF transformation $g_j^0 = (f_j^0)^{-1}$ for the j -th dimension is defined as

$$g_j^0(z_j) := \frac{g_0(z_j) - \int g_0(t) \phi\left(\frac{t - \mu_j}{\sigma_j}\right) dt}{\sqrt{\int \left(g_0(y) - \int g_0(t) \phi\left(\frac{t - \mu_j}{\sigma_j}\right) dt\right)^2 \phi\left(\frac{y - \mu_j}{\sigma_j}\right) dy}}, \quad (5.2)$$

where $\phi(\cdot)$ is the Standard Gaussian density function.

Definition 5.2. (Power Transformation) Let $g_0(t) := \text{sign}(t)|t|^\alpha$ where $\alpha > 0$ is a parameter. The power transformation for the j -th dimension is defined as

$$g_j^0(z_j) := \frac{g_0(z_j - \mu_j)}{\sqrt{\int g_0^2(t - \mu_j) \phi\left(\frac{t - \mu_j}{\sigma_j}\right) dt}}. \quad (5.3)$$

where $\phi(\cdot)$ is the Standard Gaussian density function.

These two transformations have been proposed by Liu et al. (2009) to study the performance of the original nonparanormal estimator. To comply with their simulation design, for the Gaussian CDF transformation we set $\mu_{g_0} = 0.05$ and $\sigma_{g_0} = 0.4$; for the power transformation, we set $\alpha = 3$.

To generate synthetic data, we set $d = 100$, resulting in $\binom{100}{2} + 100 = 5,050$ parameters to be estimated. The sample sizes are varied from $n = 100, 200$ to 500. Three conditions are considered, corresponding to using the power transformation, the Gaussian CDF transformation, and linear transformation (or no transformation)².

To evaluate the robustness of these methods, we consider two types of data contamination mechanisms: the *deterministic contamination* vs. *random contamination*. Let $r \in (0, 1)$ be the contamination level. For deterministic contamination we replace $\lfloor nr \rfloor$ data points with a deterministic vector $(+5, -5, +5, -5, +5, \dots)^T \in \mathbb{R}^d$, in which the numbers $+5$ and -5 occur in an alternating way. For random contamination, we randomly (according to uniform distribution) select $\lfloor nr \rfloor$ entries of each dimension and replace them with either $+5$ or -5 with equal probability. From the robustness point of way, the deterministic contamination is more malicious and can severely hurt non-robust procedures. In contrast, the random contamination is more benign and is more realistic for modern scientific data analysis.

Both the normal-score based nonparanormal estimators (**npn** and **npn-ns**) and the nonparanormal SKEPTIC estimators (**npn-spearman** and **npn-tau**) are two-step procedures. In the first step we obtain an estimate \hat{S} of the correlation matrix; in the second step we plug \hat{S} into a parametric graph estimation procedure. In this numerical study, we consider two parametric baseline procedures: (i) the graphical lasso and (ii) the Meinshausen-Bühlmann graph estimator. The former one represents the likelihood-based approach and the latter one represents the pseudo-likelihood based approach. For empirical applications, we found that the CLIME has a similar behavior to the graphical lasso, while the graphical Dantzig selector behaves similarly to the Meinshausen-Bühlmann method. Our implementations of the nonparanormal SKEPTIC, graphical lasso and Meinshausen-Bühlmann methods are available in the R package **huge**³.

Let $G = (V, E)$ be a d -dimensional graph. We denote $|E|$ to be the number of edges in the graph G . We adopt false positive and false negative rates to evaluate the graph estimation performance. Let $\hat{G}^\lambda = (V, \hat{E}^\lambda)$ be an estimated graph using the regularization parameter λ in either the graphical lasso procedure (3.12). The number of false positives when using the regularization parameter λ is

$$\text{FP}(\lambda) := \text{number of edges in } \hat{E}^\lambda \text{ not in } E \quad (5.4)$$

The number of false negatives at λ is defined as

$$\text{FN}(\lambda) := \text{number of edges in } E \text{ not in } \hat{E}^\lambda. \quad (5.5)$$

We further define the false negative rate (FNR) and false positive rate (FPR) as

$$\text{FNR}(\lambda) := \frac{\text{FN}(\lambda)}{|E|} \quad \text{and} \quad \text{FPR}(\lambda) := \text{FP}(\lambda) / \left[\binom{d}{2} - |E| \right]. \quad (5.6)$$

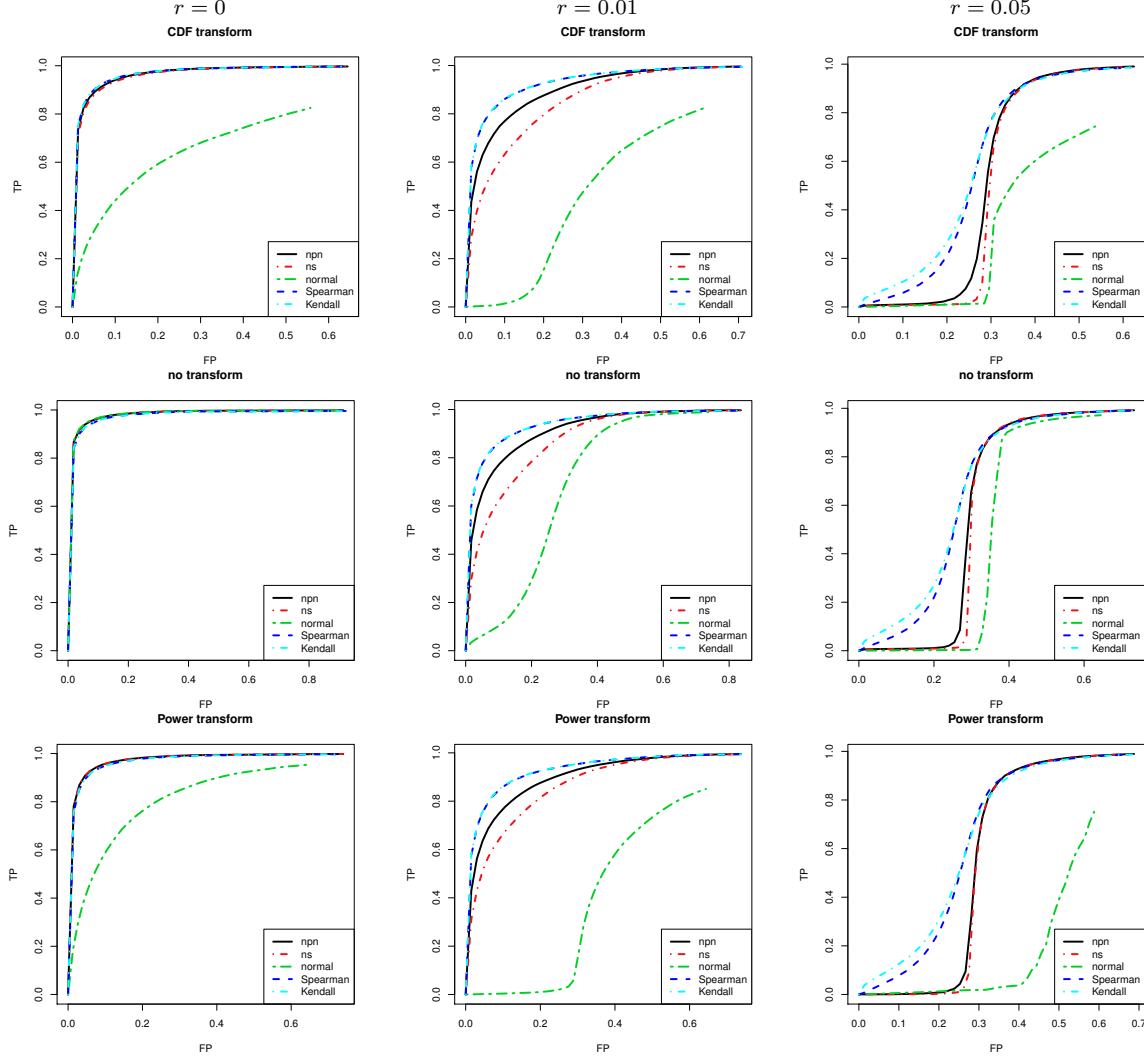


FIG 2. ROC curves for the cdf, linear and power transformations (top, middle, bottom) using the Meinshausen-Bühlmann graph estimator, with deterministic data contamination at different levels ($r=0, 0.01, 0.05$). Here $n = 200$ and $d = 100$. Note: “npn” is the original Winsorized normal-score nonparanormal estimator from Liu et al. (2009); “normal” is the naive Gaussian graph estimator; “Spearman” represents the nonparanormal SKEPTIC using Spearman’s rho; “Kendall” represents the nonparanormal SKEPTIC using Kendall’s tau; “npn-ns” represents the normal-score based nonparanormal estimator.

Let Λ be the set of all regularization parameters used to create the full path. The oracle regularization parameter λ^* is defined as

$$\lambda^* := \arg \min_{\lambda \in \Lambda} \{ \text{FNR}(\lambda) + \text{FPR}(\lambda) \}.$$

The oracle score is defined to be $\text{FNR}(\lambda^*) + \text{FPR}(\lambda^*)$. To illustrate the overall performance of the studied methods over the full paths, the averaged ROC curves for $n = 200, d = 100$

²For linear transformation, the data exactly follow the Gaussian distribution.

³<http://cran.r-project.org/web/packages/R.huge/>. The package **huge** corrects some non-convergence problem of the **glasso** package.

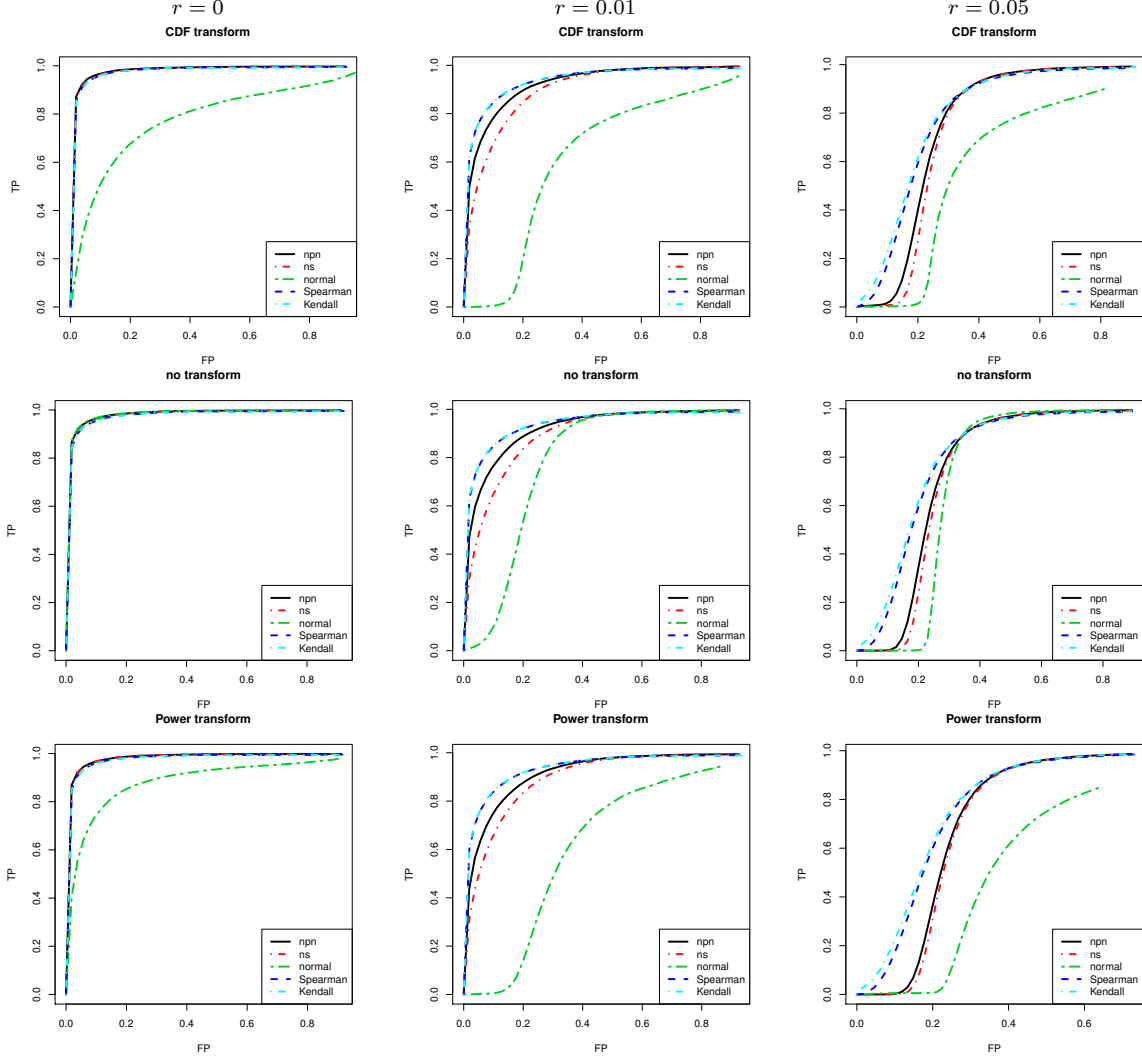


FIG 3. ROC curves for the *cdf*, linear and power transformations (top, middle, bottom) using the *glasso* graph estimator, with deterministic data contamination at different levels ($r=0, 0.01, 0.05$). Here $n = 200$ and $d = 100$. . Note: “*npn*” is the original Winsorized normal-score nonparanormal estimator from Liu et al. (2009); “*normal*” is the naive Gaussian graph estimator; “*Spearman*” represents the nonparanormal SKEPTIC using Spearman’s rho; “*Kendall*” represents the nonparanormal SKEPTIC using Kendall’s tau; “*npn-ns*” represents the normal-score based nonparanormal estimator.

over 100 trials are shown in Figures 2 to 5, using $(\text{FNR}(\lambda), 1 - \text{FPR}(\lambda))$. For each figure five curves are presented, corresponding to *npn*, *npn-tau*, *npn-spearman*, *npn-ns*, and *normal*.

Let $\text{FPR} := \text{FPR}(\lambda^*)$ and $\text{FNR} := \text{FNR}(\lambda^*)$, Tables 1 to 4 provide numerical comparisons of the three methods on datasets with the power transformation, where we repeat the experiments 100 times and report the average FPR and FNR values with the corresponding standard errors in the parenthesis.

To further illustrate the estimation efficiency loss of the nonparanormal SKEPTIC (*npn-spearman* and *npn-tau*) compared with the normal-score based estimation methods (*npn* and *npn-ns*), in Figure 6 we compare these methods on a higher dimensional Gaussian dataset

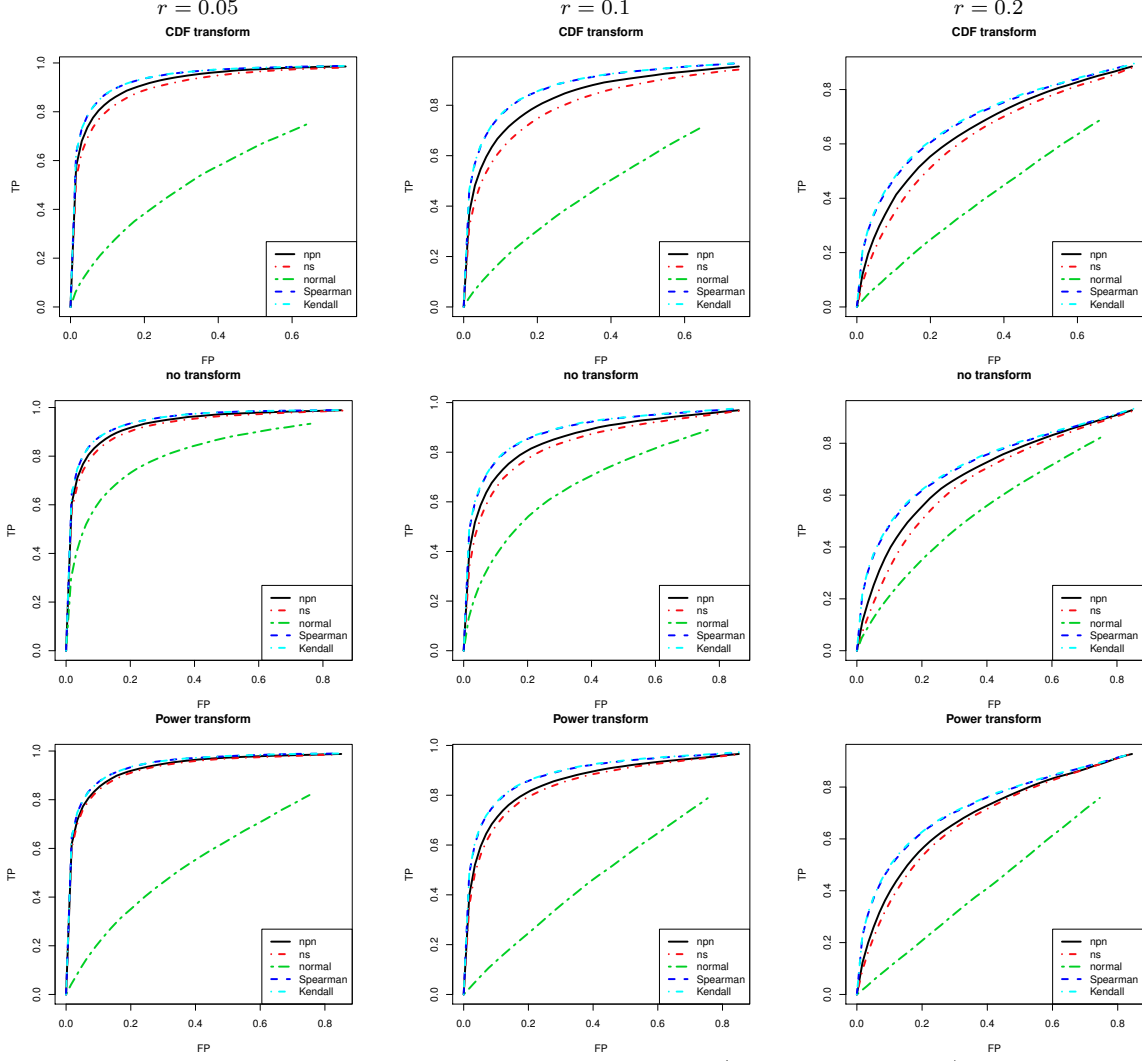


FIG 4. ROC curves for the cdf, linear and power transformations (top, middle, bottom) using the glasso graph estimator, with random data contamination at different levels ($r=0.05, 0.1, 0.2$). Here $n = 200$ and $d = 100$. . Note: “npn” is the original Winsorized normal-score nonparanormal estimator from Liu et al. (2009); “normal” is the naive Gaussian graph estimator; “Spearman” represents the nonparanormal SKEPTIC using Spearman’s rho; “Kendall” represents the nonparanormal SKEPTIC using Kendall’s tau; “npn-ns” represents the normal-score based nonparanormal estimator.

with $n = 100, d = 200$ with no outlier added in. In the following we provide detailed analysis based on these numerical simulations.

5.2.1. Non-Gaussian Data with No Outlier

From the power transformation and CDF transformation plots in Figures 2 to 5, we see that, when the contamination level $r = 0$, the performance of the nonparanormal SKEPTIC estimators (npn-spearman and npn-tau) and the previous normal-score based nonparanormal estimators (npn, and npn-ns) are comparable. In this case, all these methods significantly

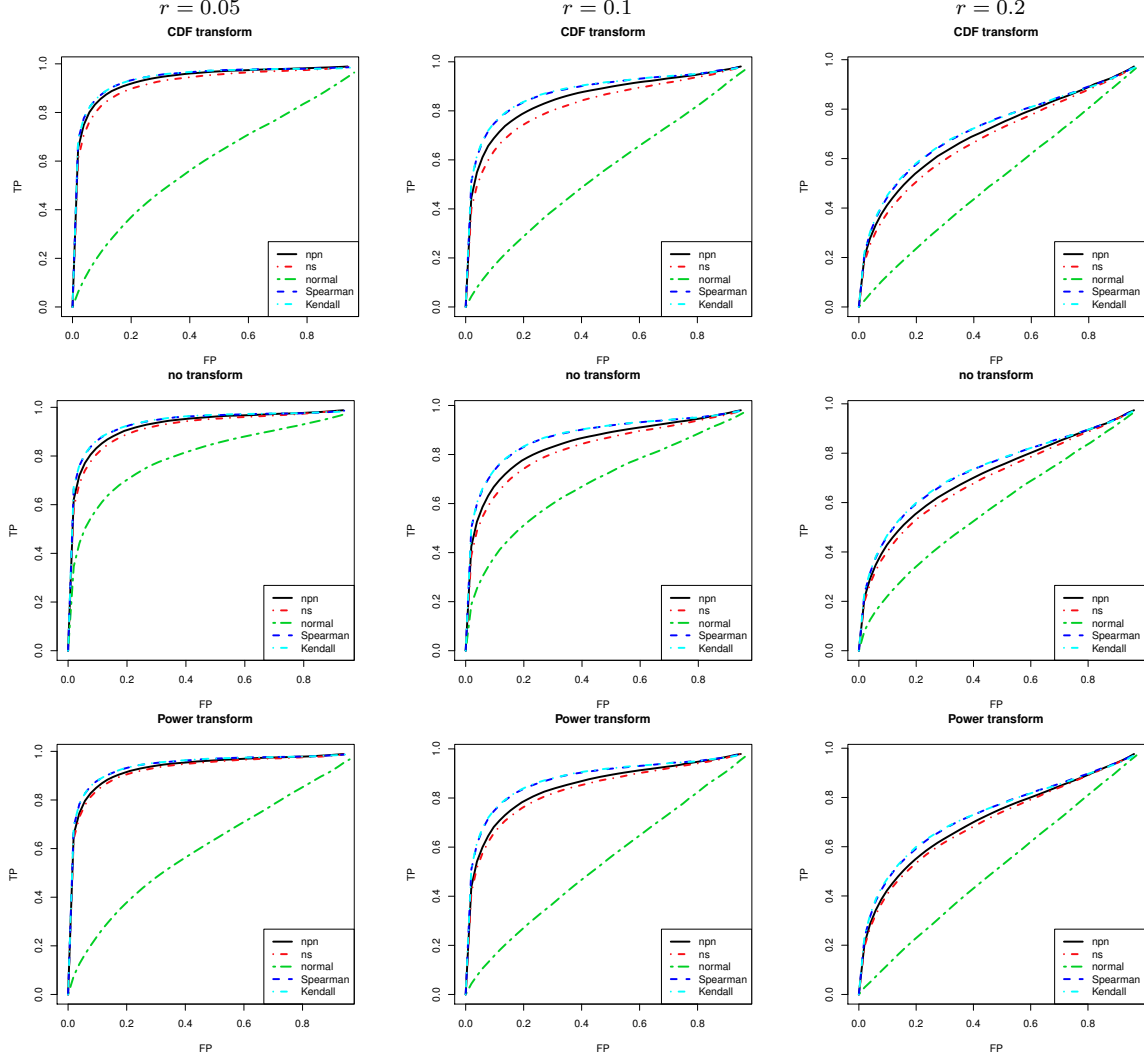


FIG 5. ROC curves for the cdf, linear and power transformations (top, middle, bottom) using the Meinshausen-Bühlmann graph estimator, with random data contamination at different levels ($r=0.05, 0.1, 0.2$). Here $n = 200$ and $d = 100$. Note: “npn” is the Winsorized normal-score nonparanormal estimator from Liu et al. (2009); “normal” is the naive Gaussian graph estimator; “Spearman” represents the nonparanormal SKEPTIC using Spearman’s rho; “Kendall” represents the nonparanormal SKEPTIC using Kendall’s tau; “npn-ns” represents the nonparanormal SKEPTIC using normal-score rank correlation coefficient.

outperform the corresponding parametric methods (the graphical lasso and Meinshausen-Bühlmann procedure).

From Tables 1 to 4, we could see that in terms of oracle FPR and FNR, npn-ns and npn seem slightly better than npn-spearman and npn-tau, though it is qualitatively undetectable based on eyeball examination of the ROC curves.

5.2.2. Non-Gaussian Data with Low Level of Outliers

When the outlier contamination level is low ($r = 0.01$ for the deterministic contamination and $r = 0.1$ for the random contamination), the performance of the nonparanomral SKEPTIC

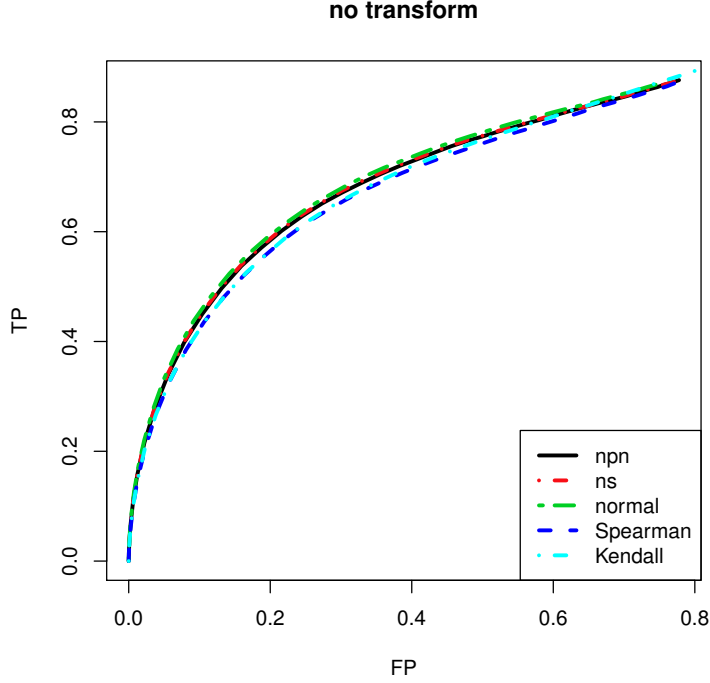


FIG 6. ROC curves for the linear transform using the glasso algorithm, with no contamination. Here $d=200$, and $n=100$. Note: “npn” is the Winsorized normal-score nonparanormal estimator from Liu et al. (2009); “normal” is the naive Gaussian graph estimator; “Spearman” represents the nonparanormal SKEPTIC using Spearman’s rho; “Kendall” represents the nonparanormal SKEPTIC using Kendall’s tau; “npn-ns” represents the nonparanormal SKEPTIC using normal-score rank correlation coefficient.

(npn-spearman and npn-tau) are significantly better than those of npn and npn-ns. Still, all these semiparametric methods significantly outperform the corresponding parametric methods (the graphical lasso and Meinshausen-Bühlmann procedure). Similar patterns can also be found based on the quantitative comparisons from Tables 1 to 4.

5.2.3. Non-Gaussian Data with Higher Level of Outliers

Again, based on the power transformation and CDF transformation plots in Figures 2 to 5, we see that when the data contamination level is higher ($r = 0.05$ for the deterministic contamination and $r = 0.20$ for the random contamination), the performance of the nonparanormal SKEPTIC (npn-spearman and npn-tau) are significantly better than those of npn and npn-ns. For this high outlier case, npn-tau outperforms npn-spearman, suggesting that the Kendall’s tau is more robust than the Spearman’s rho statistic. The parametric methods (the graphical lasso and Meinshausen-Bühlmann procedure) again perform the worst.

Unlike the previous low outlier case, the quantitative results from Tables 1 to 4 present interesting patterns. For deterministic contamination, we do not see significant improvement

TABLE 1

Quantitative comparison of the 5 methods on simulated datasets using different nonparanormal transformations. The graphs are estimated using the glasso algorithm with deterministic data contamination. Note: “npn” is the Winsorized normal-score nonparanormal estimator from Liu et al. (2009); “normal” is the naive Gaussian graph estimator; “Spearman” represents the nonparanormal SKEPTIC using Spearman’s rho; “Kendall” represents the nonparanormal SKEPTIC using Kendall’s tau; “npn-ns” represents the nonparanormal SKEPTIC using normal-score rank correlation coefficient.

tf	r	n	npn		npn-ns		normal		spearman		kendall	
			FPR(%)	FNR	FPR	FNR	FPR	FNR	FPR	FNR	FPR	FNR
cdf	0.00	100	11(2.9)	13(3.5)	11(3.1)	13(3.6)	26(6.9)	38(9.2)	11(3.4)	15(3.6)	11(3.2)	15(3.6)
		200	6(2)	5(2.1)	6(1.9)	6(2.5)	18(6.7)	32(17.2)	6(2.2)	6(2.4)	6(2.1)	6(2.4)
		500	2(1.6)	1(1.2)	3(1.7)	1(1.1)	11(4.2)	19(20.9)	3(1.6)	2(1.4)	3(1.6)	2(1.4)
	0.01	100	14(3.8)	15(3.9)	16(4.4)	15(4.5)	33(8)	38(11.4)	13(3.1)	16(3.8)	13(3.2)	16(3.9)
		200	12(3.7)	16(4.5)	24(7.8)	13(6.7)	40(9.7)	28(15.8)	10(2.7)	12(3.4)	10(2.8)	12(3.1)
		500	4(1.6)	5(2)	7(2.4)	8(2.7)	40(9.3)	17(14.2)	3(1.5)	3(1.5)	3(1.4)	3(1.6)
	0.05	100	27(2.6)	12(3.5)	26(2.4)	12(3.5)	40(10.4)	40(13)	25(2.3)	14(3.3)	27(2.9)	13(3.2)
		200	36(2)	7(2)	37(2)	7(2)	37(13.8)	35(24.4)	36(2.4)	8(2.5)	36(2.3)	8(2.7)
		500	33(1.3)	1(0.9)	33(1.2)	1(1)	43(10.7)	21(17.4)	31(1.4)	1(1)	31(1.5)	1(1.2)
normal	0.00	100	11(3.2)	13(3.7)	11(2.9)	13(3.1)	11(2.8)	12(3.2)	11(2.6)	14(3.5)	11(2.8)	15(3.5)
		200	6(2.1)	5(2)	5(2)	5(2)	5(1.5)	5(4.1)	6(2)	6(2.1)	6(2.1)	6(2.3)
		500	2(1)	1(1.1)	2(1.1)	1(1)	2(0.9)	1(0.7)	2(0.9)	1(1.2)	2(0.9)	1(1.2)
	0.01	100	14(3.3)	16(4.1)	16(4.3)	16(4.8)	25(3.3)	13(7.6)	13(3.5)	16(4)	13(3.8)	16(4.5)
		200	13(4.4)	16(4.6)	27(5.9)	11(5.6)	37(4)	6(8.2)	10(2.7)	12(3.2)	9(2.9)	12(3.3)
		500	5(2.1)	5(2.3)	7(2.3)	10(3.4)	33(2.9)	2(3.6)	3(1.2)	3(1.6)	3(1.3)	3(1.6)
	0.05	100	26(2.4)	12(3.2)	27(2.6)	12(3.3)	35(4.9)	17(7.5)	26(2.4)	13(3.4)	27(2.5)	13(3.1)
		200	37(1.9)	7(3)	37(1.9)	7(2.9)	37(5.5)	7(12.1)	36(2.4)	8(2.8)	37(2.6)	8(2.8)
		500	33(1.4)	1(1)	33(1.3)	1(1.1)	35(3.3)	5(5.8)	31(1.4)	1(1)	31(1.4)	1(1.1)
power	0.00	100	11(2.9)	13(3.4)	11(3.2)	13(3.4)	25(5)	32(6.7)	11(3.3)	14(3.6)	12(3.5)	14(3.7)
		200	6(2.7)	5(2.4)	6(2.9)	5(2.2)	19(4.2)	18(6.4)	6(2.7)	6(2.7)	6(2.6)	6(2.7)
		500	2(1.5)	1(1.1)	2(1.4)	1(1.1)	9(2.3)	8(3)	2(1.3)	1(1.3)	2(1.5)	1(1.3)
	0.01	100	14(3.5)	16(4.4)	16(3.8)	16(4.4)	33(5.2)	32(6.1)	13(3.6)	16(4.2)	13(3.3)	16(3.9)
		200	12(3.5)	17(4.3)	21(7.2)	15(7.5)	50(8.5)	23(13.1)	10(2.8)	12(3.3)	9(2.7)	12(3.5)
		500	5(1.6)	5(2)	5(1.9)	7(2.3)	40(4.5)	13(6.1)	3(1.4)	3(1.4)	3(1.3)	3(1.5)
	0.05	100	26(2.3)	12(3.1)	26(2.2)	12(3.2)	43(6.3)	41(8.7)	25(2.5)	13(3.4)	26(2.5)	13(3.3)
		200	37(2.1)	8(3.1)	37(2.1)	8(3.2)	48(6.8)	27(11.9)	36(2.5)	8(2.8)	37(2.7)	8(3.3)
		500	33(1.4)	1(1.1)	33(1.2)	1(1.8)	47(3.4)	14(5.3)	31(1.4)	1(1.2)	31(2.8)	1(3.2)

TABLE 2

Quantitative comparison of the 5 methods on simulated datasets using different nonparanormal transformations. The graphs are estimated using the Meinshausen-Bühlmann algorithm with deterministic data contamination. Note: “npn” is the Winsorized normal-score nonparanormal estimator from Liu et al. (2009); “normal” is the naive Gaussian graph estimator; “Spearman” represents the nonparanormal SKEPTIC using Spearman’s rho; “Kendall” represents the nonparanormal SKEPTIC using Kendall’s tau; “npn-ns” represents the nonparanormal SKEPTIC using normal-score rank correlation coefficient.

tf	r	n	npn		npn-ns		normal		spearman		kendall	
			FPR(%)	FNR	FPR	FNR	FPR	FNR	FPR	FNR	FPR	FNR
cdf	0.00	100	10(2.8)	15(4.2)	10(2.9)	15(4.4)	25(5.5)	44(6.4)	11(2.6)	16(4.4)	11(2.7)	16(4.4)
		200	4(1.5)	5(2.5)	5(1.7)	6(3)	20(4.6)	30(5.4)	5(1.7)	5(2.6)	5(1.9)	5(2.4)
		500	1(0.7)	1(0.8)	1(0.7)	1(1)	11(2.9)	12(3.4)	1(0.6)	1(0.9)	1(0.6)	1(0.8)
	0.01	100	12(3.5)	16(4)	14(3.3)	15(3.5)	33(7.4)	43(8)	11(3)	17(3.9)	12(3.1)	16(3.9)
		200	15(3.4)	12(3.5)	21(3.4)	12(3.6)	38(4.6)	29(5.1)	10(3.3)	13(3.6)	10(3.1)	12(3.4)
		500	4(1.7)	4(2.9)	6(2.4)	5(3.3)	39(3.4)	14(4.6)	2(1.4)	2(2.2)	2(1.2)	2(2.2)
	0.05	100	22(2.5)	14(3.3)	23(2.5)	15(3.5)	39(7)	43(7.9)	21(3.2)	16(4.1)	22(3)	16(4.2)
		200	35(2.8)	9(3.5)	35(3)	9(3.5)	42(4.3)	28(5.7)	32(3.2)	11(4.1)	33(3.5)	11(3.8)
		500	27(2.3)	3(1.9)	29(1.9)	3(1.9)	46(4.2)	15(4.6)	21(2.7)	4(2.3)	20(2.6)	4(2.4)
normal	0.00	100	10(2.8)	15(3.5)	10(2.7)	14(3.4)	9(2.5)	14(3.2)	11(2.8)	16(3.6)	11(2.6)	16(3.4)
		200	4(1.5)	5(1.9)	4(1.5)	5(1.8)	4(1.6)	5(2)	5(1.5)	6(2.4)	5(1.6)	6(2.3)
		500	1(0.6)	1(1.1)	1(0.6)	1(1.1)	1(0.6)	1(1.1)	1(0.6)	1(1.1)	1(0.6)	1(1.3)
	0.01	100	12(2.9)	16(3.9)	14(3.5)	16(4.1)	22(3)	15(3.7)	12(3.5)	17(4)	11(3.1)	18(4.2)
		200	16(3.8)	13(4.3)	23(3.7)	11(4.1)	34(2.3)	7(2.7)	10(3.4)	13(4)	10(3.1)	13(3.8)
		500	4(1.5)	4(1.9)	7(2.2)	5(2.2)	23(2.4)	4(2.2)	2(1.1)	2(1.4)	2(1)	2(1.5)
	0.05	100	23(2.8)	15(3.3)	23(2.5)	15(3.6)	30(3.9)	20(4.1)	22(3.1)	16(4.1)	21(3.3)	17(3.6)
		200	35(2.6)	9(3.2)	36(2.6)	8(3.1)	37(2.1)	6(2.2)	32(2.9)	10(3.4)	33(3)	10(3.3)
		500	27(2.1)	2(1.5)	29(1.9)	2(1.5)	33(2)	4(1.8)	21(2.5)	4(2.1)	20(2.7)	4(2.3)
power	0.00	100	10(2.9)	15(3.8)	10(2.9)	14(3.9)	18(4.2)	33(5.3)	11(3.1)	16(4.2)	10(3.3)	17(4.2)
		200	4(1.6)	5(1.9)	4(1.7)	5(1.9)	14(2.9)	18(4.1)	5(1.5)	6(2.2)	5(1.6)	6(2.2)
		500	1(0.6)	1(0.7)	1(0.5)	1(0.7)	7(1.8)	6(2)	1(0.5)	1(0.8)	1(0.6)	1(0.7)
	0.01	100	13(2.9)	16(3.9)	14(2.9)	16(4.4)	26(5.5)	37(6.7)	12(2.8)	18(3.9)	12(3)	17(3.3)
		200	17(4)	13(4.6)	21(4)	12(4.2)	45(4.6)	23(5.7)	11(3.1)	13(3.8)	10(3.3)	13(3.9)
		500	4(1.5)	4(2.4)	5(2.1)	5(2.8)	36(4.2)	13(6.4)	2(1.1)	2(1.9)	2(1.4)	2(2)
	0.05	100	22(2.8)	15(3.3)	23(2.5)	15(3.3)	41(9.8)	42(11)	20(2.9)	17(3.6)	22(2.9)	17(3.6)
		200	35(2.8)	9(4.1)	35(2.6)	9(3.9)	50(5.4)	24(7.5)	32(2.9)	10(3.4)	33(2.9)	10(3.9)
		500	27(1.9)	2(1.7)	28(2.1)	2(1.7)	45(3.7)	14(4.4)	20(2.4)	4(2.3)	20(2.8)	4(2.5)

of the npn-spearman and npn-tau over npn and npn-ns in terms of oracle FPR and FNR. At the first sight this seems counter-intuitive since the corresponding ROC curves suggest that

TABLE 3

Quantitative comparison of the 5 methods on simulated datasets using different nonparanormal transformations. The graphs are estimated using the glasso algorithm with random data contamination. Note: “npn” is the Winsorized normal-score nonparanormal estimator from Liu et al. (2009); “normal” is the naive Gaussian graph estimator; “Spearman” represents the nonparanormal SKEPTIC using Spearman’s rho; “Kendall” represents the nonparanormal SKEPTIC using Kendall’s tau; “npn-ns” represents the nonparanormal SKEPTIC using normal-score rank correlation coefficient.

tf	r	n	npn		npn-ns		normal		spearman		kendall	
			FPR(%)	FNR	FPR	FNR	FPR	FNR	FPR	FNR	FPR	FNR
cdf	0.05	100	16(3.6)	24(4.9)	17(4.4)	26(5.7)	27(12.9)	57(13.3)	16(3.9)	23(4.8)	16(4.1)	23(5)
		200	10(2.2)	12(3)	11(2.6)	14(3.6)	26(10.9)	51(12.5)	10(2.8)	11(3.2)	9(2.6)	11(3.3)
		500	4(2.1)	4(2.5)	5(2.1)	6(2.7)	22(8.3)	40(13.9)	4(2.1)	4(2.2)	4(2)	4(2.1)
	0.10	100	19(5)	35(6.2)	20(4.9)	37(6.3)	30(17.4)	59(18)	17(4.8)	33(6.1)	18(4.8)	33(6.2)
		200	15(3.8)	21(4.6)	16(3.9)	25(5.1)	29(13.2)	56(13.3)	13(3.3)	18(4.6)	13(3.5)	18(4.5)
		500	7(2.3)	9(2.7)	9(2.4)	12(3.1)	27(11.3)	50(13)	6(1.9)	7(2.2)	6(2.1)	6(2.2)
	0.20	100	28(7.9)	47(8.2)	29(7.5)	48(8.2)	30(19.2)	64(20.4)	24(7.8)	50(8.2)	24(7.9)	49(7.8)
		200	24(6.7)	39(7.5)	28(6.7)	39(6.9)	31(17.8)	61(18.6)	20(5.8)	37(6.7)	19(5.7)	37(6)
		500	17(3.5)	23(4.6)	20(4.7)	28(5)	34(15.4)	54(15.6)	13(3.6)	19(4.4)	12(3.3)	19(4.2)
normal	0.05	100	15(3.5)	25(4.6)	16(4.6)	26(4.7)	23(6.3)	38(6.7)	15(3.6)	23(4.6)	14(3.2)	24(4.6)
		500	5(2.4)	4(1.9)	5(2.4)	5(2)	10(2.7)	12(3.7)	4(2.2)	3(1.7)	4(2.2)	3(1.6)
		200	10(2.3)	13(3.4)	11(2.5)	14(3.4)	16(4.3)	27(8.4)	9(2.5)	11(3)	9(2.2)	11(3.2)
	0.10	100	19(4.8)	35(6)	20(5.4)	37(6.3)	28(10.2)	48(9.6)	19(4.6)	32(5.2)	18(4.6)	32(5.3)
		200	14(4)	22(4.5)	15(3.8)	25(4.2)	24(6.5)	40(7.1)	13(3)	18(4.2)	12(3.1)	18(4.3)
		500	8(2.1)	9(2.7)	10(2.5)	11(3.2)	19(4.6)	24(4.8)	6(1.9)	7(2.4)	6(2.2)	6(2.3)
	0.20	100	28(7.6)	48(7.8)	30(9)	47(8.8)	35(18)	53(17.5)	24(7.6)	49(7.6)	24(7)	49(7.2)
		200	25(5.1)	37(6.5)	30(6.5)	36(7)	32(11.4)	50(11.6)	19(5.3)	37(6.3)	18(4.8)	38(5.7)
		500	18(4)	23(5.2)	22(4.8)	25(5.4)	27(7.4)	41(8.2)	13(3.8)	19(4.2)	13(3.5)	19(4.2)
power	0.05	100	15(4.5)	25(5.7)	16(4.4)	25(5)	33(13.2)	55(13.9)	15(4.1)	23(4.8)	16(4.3)	22(5.1)
		200	10(3.2)	13(3.7)	10(3.1)	14(3.5)	30(8.4)	52(8.9)	9(2.8)	12(3.4)	9(2.7)	11(3.2)
		500	4(2.2)	4(1.8)	5(2)	5(1.9)	28(6.9)	39(8.1)	4(2)	3(1.7)	4(2.1)	3(1.7)
	0.10	100	20(4.9)	35(5.7)	20(6)	36(6.4)	38(22.2)	56(22.5)	18(5.2)	32(5.7)	18(5.1)	32(5.8)
		200	14(4.1)	22(5.2)	16(3.8)	23(5.1)	39(16.4)	52(17.3)	13(3.9)	19(4.5)	12(3.7)	18(4.1)
		500	7(2.2)	9(2.7)	8(2.2)	10(2.9)	37(11.7)	46(12.1)	6(1.7)	6(2.2)	5(1.7)	6(2.1)
	0.20	100	27(7.7)	48(9.5)	30(8.4)	47(9.9)	42(24.8)	54(25.6)	22(7.3)	50(8.9)	23(8)	49(9.2)
		200	24(6)	38(7.2)	27(5.9)	38(7.3)	41(24.4)	54(25)	20(4.7)	37(5.5)	19(5.1)	36(5.8)
		500	18(4)	23(4.8)	20(4.2)	24(5.3)	41(16.9)	51(17.7)	13(3.6)	19(4.3)	12(3.1)	19(4.3)

TABLE 4

Quantitative comparison of the 5 methods on simulated datasets using different nonparanormal transformations. The graphs are estimated using the Meinshausen-Bühlmann algorithm with random data contamination. Note: “npn” is the Winsorized normal-score nonparanormal estimator from Liu et al. (2009); “normal” is the naive Gaussian graph estimator; “Spearman” represents the nonparanormal SKEPTIC using Spearman’s rho; “Kendall” represents the nonparanormal SKEPTIC using Kendall’s tau; “npn-ns” represents the nonparanormal SKEPTIC using normal-score rank correlation coefficient.

tf	r	n	npn		npn-ns		normal		spearman		kendall	
			FPR(%)	FNR	FPR	FNR	FPR	FNR	FPR	FNR	FPR	FNR
cdf	0.05	100	15(3.7)	27(4.3)	15(3.5)	30(4.5)	29(16.1)	60(15.8)	13(3.3)	27(4.4)	14(3.2)	26(4.3)
		200	9(2.4)	13(3.1)	10(2.7)	15(4.1)	27(9.7)	53(10.5)	9(2.5)	11(3.4)	8(2.7)	11(3.3)
		500	3(1.5)	4(1.8)	4(1.4)	5(2.2)	21(5.7)	42(6.8)	3(1.3)	3(1.8)	3(1.2)	3(1.8)
	0.10	100	18(4.7)	40(5.4)	18(5.7)	42(6.6)	38(21.6)	55(21.7)	18(5)	37(5.8)	17(5.1)	36(5.6)
		200	13(3.6)	25(5.3)	15(3.9)	28(5.6)	32(14.2)	56(14)	12(3.2)	21(5.2)	12(3.2)	21(5)
		500	7(2.4)	10(2.9)	9(2.9)	14(3.4)	24(9.2)	53(10.6)	5(1.8)	6(2.6)	5(1.5)	6(2.6)
	0.20	100	22(8.2)	55(8.2)	22(7.8)	56(8.4)	50(31.4)	45(31)	22(7.7)	54(9)	22(7)	53(8)
		200	19(6.5)	45(7.5)	19(7.2)	48(8)	36(23.7)	57(23.5)	19(6.2)	40(7.3)	19(5.5)	41(7.1)
		500	14(4.1)	28(5)	15(3.9)	35(5.6)	29(16.3)	57(15.7)	12(3)	21(4.4)	12(3.4)	21(4.6)
normal	0.05	100	14(3.6)	29(4.9)	14(3.6)	30(4.7)	19(5.8)	45(6.8)	14(4)	26(5.3)	13(4.3)	26(5.2)
		200	10(2.9)	14(3.5)	10(2.9)	16(4.2)	15(4.4)	31(5)	9(2.7)	12(3.1)	8(2.4)	12(2.9)
		500	3(1.3)	3(1.6)	4(1.5)	4(1.9)	8(2.7)	14(3.3)	3(1.2)	3(1.7)	3(1.1)	3(1.6)
	0.10	100	17(5)	41(6.3)	17(4.6)	43(6.2)	20(6.9)	59(7.9)	18(5.2)	37(6.3)	18(4.6)	35(5.8)
		200	14(3.8)	25(5.2)	14(4.2)	29(5.6)	19(6.6)	47(6.9)	12(3.1)	21(4.4)	12(3.2)	21(4.6)
		500	7(2.2)	10(2.9)	8(2.6)	13(3.2)	14(4.2)	30(5.8)	5(1.7)	7(2.4)	5(1.7)	7(2.5)
	0.20	100	23(9.1)	54(9.3)	22(8.8)	56(9.2)	28(18)	61(18.1)	22(8.4)	53(8.4)	23(8.6)	52(8.8)
		200	19(5.8)	44(6.7)	19(5.9)	47(6.6)	23(10)	60(10.2)	19(5.7)	40(7)	19(6)	39(7.5)
		500	14(3.9)	29(4.9)	14(4.2)	33(6)	20(7.1)	48(8.4)	13(3.7)	20(4.5)	12(3.2)	20(4.2)
power	0.05	100	15(4.2)	28(4.9)	15(3.9)	29(5)	30(13.7)	58(14.4)	14(4.3)	26(5.1)	15(4)	25(4.8)
		200	9(2.5)	14(3.9)	9(2.6)	15(3.9)	27(10.4)	52(10.2)	8(2.6)	12(3.2)	8(2.2)	12(3.1)
		500	3(1.3)	3(1.5)	3(1.3)	4(1.6)	20(6.2)	44(7.2)	3(1.1)	2(1.4)	2(1)	2(1.3)
	0.10	100	18(5.2)	40(5.1)	18(5.4)	42(5.6)	41(25.4)	52(25)	17(5)	37(5.8)	17(4.8)	36(5.1)
		200	14(3.9)	25(5.1)	14(3.9)	27(5.6)	33(20)	57(19.5)	12(2.7)	20(4.4)	12(3.4)	20(4.3)
		500	7(1.9)	10(2.9)	7(2.3)	11(3)	26(11.3)	55(13)	5(1.7)	7(2.2)	5(1.6)	6(2.1)
	0.20	100	22(6.9)	55(8.4)	22(7.4)	56(8.7)	46(26.9)	48(26.9)	21(7.4)	54(8.3)	22(7.2)	52(8.4)
		200	19(5.9)	44(7.1)	19(6.4)	46(7.3)	43(25.5)	51(25.5)	19(6.1)	40(7.2)	18(4.9)	40(6.2)
		500	13(4.1)	27(5.7)	14(4.8)	29(5.7)	35(18.6)	56(19.3)	13(3.4)	20(4.7)	12(3.4)	19(4.5)

npn-spearman and **npn-tau** are globally better than **npn** and **npn-ns**. The main reason for such a result is that the oracle score point happens to be coincide with the intersecion point of different ROC curves. On the other hand, for random contamination setting, we see that the performance of **npn-spearman** and **npn-tau** uniformly dominate that of the **npn** and **npn-ns**.

5.2.4. *Gaussian Data with No Outlier*

From the linear transformation plot in Figures 2 to 5, we see that when the outlier contamination level $r = 0$ the performance of all these methods are comparable. Based on Tables 1 to 4, we could see that in terms of oracle FPR and FNR, **normal**, **npn-ns** and **npn** are slightly better than **npn-spearman** and **npn-tau**. This result suggests that there is very tiny efficiency loss of the nonparanormal SKEPTIC for truly Gaussian data (though this loss seems negligible). Such an efficiency loss is visualized by Figure 6 where $n = 100$ and $d = 200$.

5.2.5. *Gaussian Data with Low and Higher Levels of Outliers*

From the linear transformation plot in Figures 2 to 5, we see that when the outlier contamination level $r > 0$, the performance of the parametric methods like the graphical lasso immediately break down. The main reason is that these methods are based on the Pearson’s correlation matrix, which is very sensitive to outliers. In contrast, the other semiparametric methods (**npn-spearman**, **npn-tau**, **npn-ns**, and **npn**) are more resistant to outliers. Among them, **npn-tau** is the most robust one and **npn-spearman** behaves very similarly. Both methods outperform **npn**, which further outperforms **npn-ns**.

In summary, these simulation results illustrate an interesting tradeoff between statistical efficiencies and estimation robustness. In general, both **npn-spearman** and **npn-tau** have very good overall performance. In practice, which method to use should be determined by our prior knowledge about the data. For example, for high-throughput genomics datasets, we believe that using **npn-spearman** and **npn-tau** are more beneficial than using some less robust methods like **npn-ns**. In contrast, if we believe the data is free of outlier, a normal-score based method like **npn** could be a good choice.

5.3. *Gene Expression Data*

We compare different methods on a large genomics dataset. In this study, we collect in total 13,182 publicly available microarray samples from Affymetrixs HGU133a platform. These samples are downloaded from GEO and Array Express. Our dataset contains 2,717 tissue types (e.g., lung cancer, stem cell etc.). For each array sample, there are 22,283 probes, corresponding to 12,719 genes. To the best of our knowledge, this is thus far the largest microarray gene expression dataset that has been collected.

The main purpose of this study is to estimate the conditional independence graphs over different genes and different tissue types. To estimate the gene graph, we treat the 13,182

arrays as independent observations and the expression value of each gene as a random variable. To estimate the tissue graph, we average all the arrays belonging to the same tissue type and treat this tissue type expression as a random variable. In this setting the 12,719 gene expressions are treated as independent observations. Though it is obvious that both the genes and tissue types are not independent, we simply adopt this approach as our working procedure. This is consistent with the current state-of-the-art genomics practice.

Two major challenges for conducting statistical analysis on large-scale integrated datasets are data cleaning and batch/lab effects removal. We conduct surrogate variable analysis (Leek and Storey, 2007) on this data to remove batch effects and normalize the data from different labs. Since the main purpose of this paper is to compare different methods on empirical datasets. We mainly focus on presenting the differential graphs between different methods. The detailed data preprocessing protocols and the scientific implications of the obtained results will be reported elsewhere.

We first screen out all the genes whose marginal standard deviation is below a given threshold. Such a procedure provides us a list of 2,000 genes who vary the most across different array samples. To estimate the gene graph, we first calculate the full regularization path for 100 tuning parameters using the **nnp-spearman** and automatically select the tuning parameter using the a stability based approach named StARS (Liu et al., 2010). The delivered graph contains 1,557 edges. We then examine the full regularization paths of the other graph estimation methods and pick the graph that has closest sparsity level as this graph.

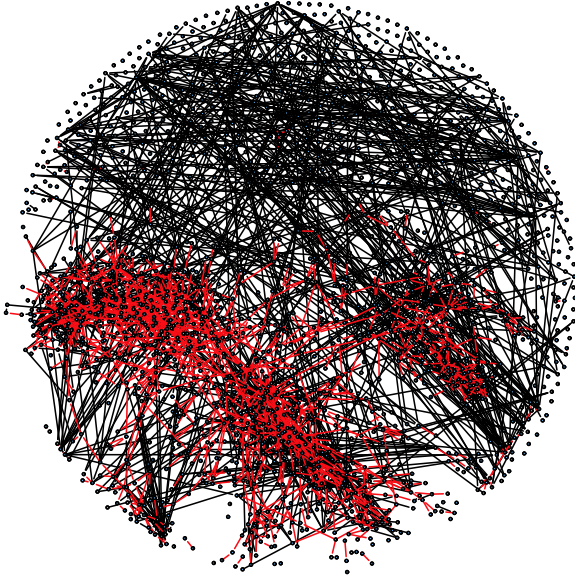
To estimate the tissue network, we first remove all the data for 3 tissue types which have less than 5 replications. So we end up studying the relationships of 2,714 tissue types. We only use the 2,000 filtered out genes to estimate the tissue network. After averaging the array samples belonging to the same tissue type, we obtain a final data matrix with size $2,000 \times 2,714$. The remaining procedure of estimating the tissue graph is the same as that of estimating the gene graph. Some summary statistics of the estimated gene and tissue graphs are presented in Table 5.

TABLE 5

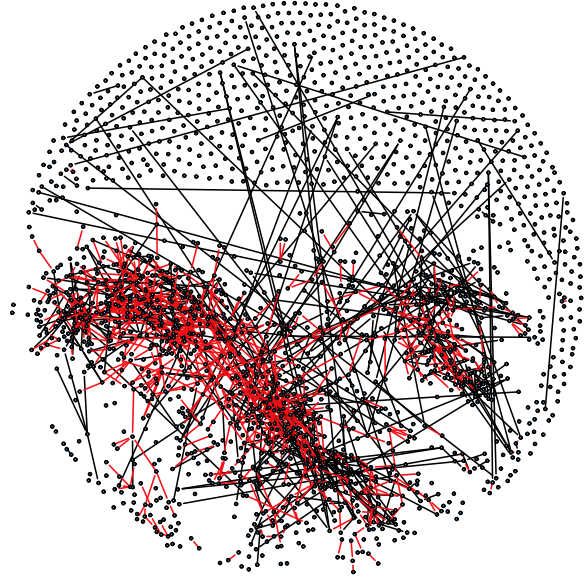
Some summary statistics of the HGU133a platform data networks learned at the gene and tissue levels. Note: GA:= normal; SP:=spearman; NS:= npn-ns. $A > B$ means the number of edges only appear in the estimated graph of A, but not in that of B; $A < B$ is on the contrary.

Network	dim	Edge No.			Edge diff			
		spearman	normal	nnp-ns	SP > GA	SP < GA	SP > NS	SP < NS
Tissue	2714	2639	2379	2478	602	342	307	146
Gene	2000	1557	1550	1411	1235	1228	691	545

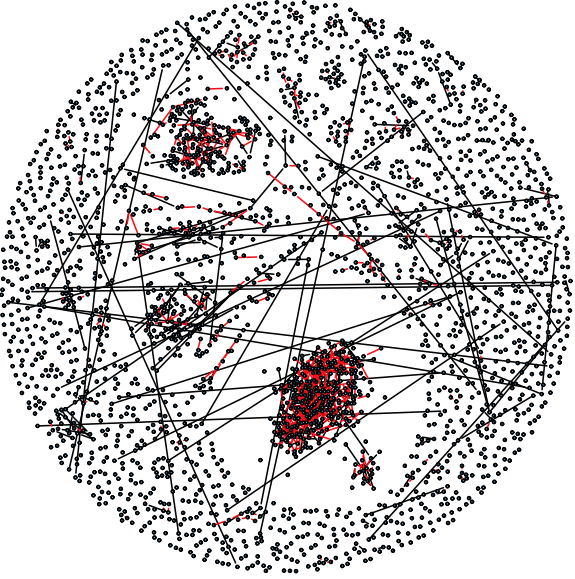
From Table 5 we see that the estimated tissue graph is denser than the gene graph. Since both graphs contain around 2,000 nodes with more than 1,500 edges, it is not very



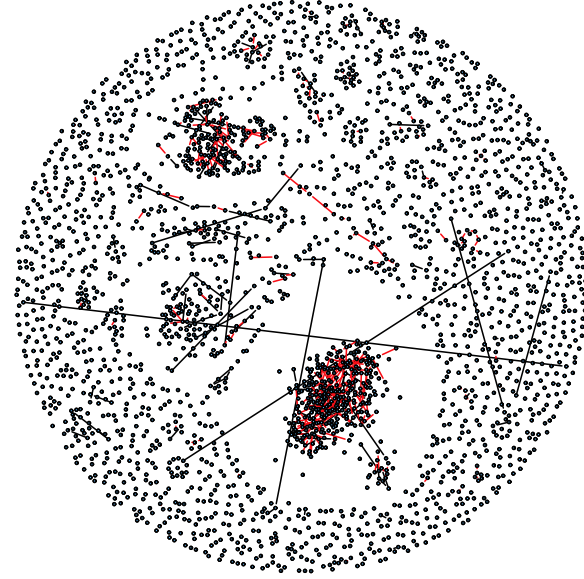
(a) Differential gene network (nnp-sp vs. normal)



(b) Differential gene network (nnp-sp vs. nnp-ns)



(c) Differential tissue network (nnp-sp vs. normal)



(d) Differential tissue network (nnp-sp vs. nnp-ns)

FIG 7. Differential gene networks between different methods. For A vs. B , the red color represent the edges that only present in A but not in B , the black color represent the edges that only present in B but not in A . (These graphics are best visualized in color).

informative to visualize these estimated graphs. Instead we are interested in understanding the differential graphs.

For example, at the gene level, the **npn-sp** graph contains 1,235 edges that are not in the **normal** graph. In contrast, the **normal** graph contains 1,228 edges that are not in the **npn-sp** graph. Since there are $1,235/1,557 \approx 80\%$ edges in **npn-sp** that are not present in the **normal** graph, this data should be highly non-Gaussian. When we further compare the **npn-sp** gene graph with the **npn-ns** graph, we found that there are $691/1,557 \approx 45\%$ edges that are not present in the **npn-ns** graph, suggesting that this data may contain high levels of outliers. Since this dataset is integrated from many sources, it's indeed quite noisy.

Compared with the gene graphs, the tissue graphs present an interesting pattern. Even though the delivered tissue graphs are much denser than the gene graphs, there are only $602/2,714 \approx 22\%$ **npn-sp** edges that are not present in the **normal** graph. Also, there are only $342/2,639 \approx 12\%$ edges in the **normal** graph that are not in the **npn-sp** graph. Such a result suggests that the data are still non-Gaussian. However, at the tissue level the data seems contain much stronger signal than that at the gene level (This may also be caused by possible uninterpreted lab effects). The similar conclusion can be drawn when we compare the **npn-spearman** tissue graph with the **npn-ns** tissue graph. For better visualization, we plot the differential graphs in Figure 7. These plots visualize the difference between the estimated graphs and double confirm the above analysis.

6. Conclusions

Most methods for estimating high dimensional undirected graphs rely on the normality assumption. To weaken this overly restrictive parametric assumption, we propose the *non-paranormal* SKEPTIC, an improved estimator that obviates the need to explicitly estimate the marginal transformations, which greatly improves the statistical rate of convergence to within logarithmic factors of the optimal parametric rate. Our analysis is non-asymptotic, and the obtained rate is minimax optimal over certain model classes. The nonparanormal SKEPTIC can thus be used as a safe replacement of Gaussian estimators, even when the data are truly Gaussian. Besides theoretical analysis, extensive numerical simulations and empirical data analysis are also provided to illustrate the usefulness of our methods. The R language software package **huge** implementing the proposed procedures is available on the Comprehensive R Archive Network: <http://cran.r-project.org/>.

Acknowledge

We thank David Donoho for very constructive comments and helpful discussions.

Appendix A: Proofs of Main Results

In this section we provide technical proofs. In the following we first prove Theorem 4.2 due to its simplicity. We then use this result to prove Theorem 4.1.

A.1. Proof of Proposition 3.1

Proof. The result on τ_{jk} directly follows from the definition of τ_{jk} .

Here we prove the result holds for ρ_{jk} . Since $F_j(X_j) \sim \text{Uniform}[0, 1]$, we have $\rho_{jk} = 12\mathbb{E}[F_j(X_j)F_k(X_k)] - 3$. We can also easily show that

$$\mathbb{E}[1 - F_j(X_j)(1 - F_k(X_k))] = \mathbb{E}[F_j(X_j)F_k(X_k)].$$

Moreover, we have

$$\begin{aligned} \mathbb{E}[F_j(X_j)F_k(X_k)] & \quad (A.1) \\ &= \mathbb{E}\left[\mathbb{P}\left(X_j^{(2)} < X_j^{(1)} \mid X_j^{(1)}\right) \mathbb{P}\left(X_k^{(3)} < X_k^{(1)} \mid X_k^{(1)}\right)\right] \\ &= \mathbb{E}\left[\mathbb{E}\left(I(X_j^{(2)} < X_j^{(1)}, X_k^{(3)} < X_k^{(1)}) \mid X_j^{(1)}, X_k^{(1)}\right)\right]. \end{aligned}$$

Similarly,

$$\begin{aligned} \mathbb{E}[(1 - F_j(X_j))(1 - F_k(X_k))] & \quad (A.2) \\ &= \mathbb{E}\left[\mathbb{P}\left(X_j^{(2)} > X_j^{(1)} \mid X_j^{(1)}\right) \mathbb{P}\left(X_k^{(3)} > X_k^{(1)} \mid X_k^{(1)}\right)\right] \\ &= \mathbb{E}\left[\mathbb{E}\left(I(X_j^{(2)} > X_j^{(1)}, X_k^{(3)} > X_k^{(1)}) \mid X_j^{(1)}, X_k^{(1)}\right)\right]. \end{aligned}$$

Combining (A.1) and (A.2), we obtain

$$\mathbb{E}[F_j(X_j)F_k(X_k)] = \frac{1}{2}\mathbb{E}[F_j(X_j)F_k(X_k)] + \frac{1}{2}\mathbb{E}[(1 - F_j(X_j))(1 - F_k(X_k))] \quad (A.3)$$

$$= \frac{1}{2}\mathbb{P}((X_j^{(1)} - X_j^{(2)})(X_k^{(1)} - X_k^{(3)}) > 0) \quad (A.4)$$

$$= \frac{1}{2}\mathbf{C}(j, 1, 2; k, 1, 3). \quad (A.5)$$

Therefore, we have

$$\rho_{jk} = 12\mathbb{E}[F_j(X_j)F_k(X_k)] - 3 \quad (A.6)$$

$$= 3(2\mathbf{C}(j, 1, 2; k, 1, 3) - 1) \quad (A.7)$$

$$= 3\mathbf{C}(j, 1, 2; k, 1, 3) - 3\mathbf{D}(j, 1, 2; k, 1, 3).$$

The last equality directly follows from the fact that $\mathbf{C}(j, 1, 2; k, 1, 3) = 1 - \mathbf{D}(j, 1, 2; k, 1, 3)$. \square

A.2. Proof of Theorem 4.2

Proof. It is easy to see that $\hat{\tau}_{jk}$ is an unbiased estimator of τ_{jk} : $\mathbb{E}\hat{\tau}_{jk} = \tau_{jk}$. We have

$$\mathbb{P}\left(\left|\hat{S}_{jk}^{\tau} - \Sigma_{jk}^0\right| > t\right) \quad (\text{A.8})$$

$$= \mathbb{P}\left(\left|\sin\left(\frac{\pi}{2}\hat{\tau}_{jk}\right) - \sin\left(\frac{\pi}{2}\tau_{jk}\right)\right| > t\right) \quad (\text{A.9})$$

$$\leq \mathbb{P}\left(\left|\hat{\tau}_{jk} - \tau_{jk}\right| > \frac{2}{\pi}t\right). \quad (\text{A.10})$$

Since $\hat{\tau}_{jk}$ can be written in the form of U-statistic:

$$\hat{\tau}_{jk} = \frac{2}{n(n-1)} \sum_{1 \leq i < i' \leq n} K_{\tau}(x^i, x^{i'}), \quad (\text{A.11})$$

where

$$K_{\tau}(x^i, x^{i'}) = \text{sign}\left(x_j^i - x_j^{i'}\right)\left(x_k^i - x_k^{i'}\right)$$

is a kernel bounded between -1 and 1 . Using the Hoeffding's inequality for U-statistic, we get

$$\mathbb{P}\left(\sup_{j,k} \left|\hat{S}_{jk}^{\tau} - \Sigma_{jk}^0\right| > t\right) \leq d^2 \exp\left(-\frac{nt^2}{2\pi^2}\right). \quad (\text{A.12})$$

We then obtain (4.4). □

A.3. Proof of Theorem 4.1

Proof. The main difficulty of this analysis is that the Spearman's rho static is over rank variables which depend on all the samples. To handle this issue, we first rewrite the rho-statistic in a different form (see Page 318, Eq (9.21) of Hoeffding (1948))

$$\hat{\rho}_{jk} = \frac{3}{n^3 - n} \sum_{i=1}^n \sum_{s=1}^n \sum_{t=1}^n \text{sign}(x_j^i - x_j^s)(x_k^i - x_k^t) \quad (\text{A.13})$$

$$= \frac{n-2}{n+1} U_{jk} + \frac{3}{n+1} \hat{\tau}_{jk}. \quad (\text{A.14})$$

where $\hat{\tau}_{jk}$ is the Kenadall's tau statistic and

$$U_{jk} = \frac{3}{n(n-1)(n-2)} \sum_{i \neq s \neq t} \text{sign}(x_j^i - x_j^s)(x_k^i - x_k^t). \quad (\text{A.15})$$

is a 3rd-order U-statistic with bounded but asymmetric kernel.

Let $0 < \alpha < 1$. We have

$$\mathbb{P} \left(\sup_{jk} |\hat{\rho}_{jk} - \mathbb{E}\hat{\rho}_{jk}| > \frac{2c}{\pi} \sqrt{\frac{\log d}{n}} \right) \leq \underbrace{d^2 \mathbb{P} \left(|U_{jk} - \mathbb{E}U_{jk}| > \frac{2\alpha c}{\pi} \sqrt{\frac{\log d}{n}} \right)}_{T_1(\alpha)} + T_2(\alpha)$$

where

$$T_2(\alpha) = d^2 \mathbb{P} \left(\frac{6}{n+1} > \frac{2}{\pi} (1-\alpha)c \sqrt{\frac{\log d}{n}} \right) = 0 \quad (\text{A.16})$$

whenever $n \geq \frac{9\pi^2}{(1-\alpha)^2 c^2 \log d}$.

Without loss of generality, we assume n can be divided by 3. Using the Hoeffding's inequality with asymmetric kernels (Hoeffding, 1963),

$$T_1(\alpha) = d^2 \mathbb{P} \left(|U_{jk} - \mathbb{E}U_{jk}| > \frac{2\alpha c}{\pi} \sqrt{\frac{\log d}{n}} \right) \quad (\text{A.17})$$

$$\leq 2d^2 \exp \left(-\frac{2}{9\pi^2} \alpha^2 c^2 \left\lfloor \frac{n}{3} \right\rfloor \cdot \frac{\log d}{n} \right) \quad (\text{A.18})$$

$$= 2 \exp \left(2 \log d - \frac{2}{27\pi^2} \alpha^2 c^2 \log d \right). \quad (\text{A.19})$$

Let

$$c = \frac{3\sqrt{6}\pi}{\alpha}. \quad (\text{A.20})$$

Therefore, whenever $n \geq \frac{1}{6 \log d} \left(\frac{\alpha}{1-\alpha} \right)^2$, with probability at least $1 - 2d^{-2}$, we have

$$\sup_{jk} |\hat{\rho}_{jk} - \mathbb{E}\hat{\rho}_{jk}| \leq \frac{6\sqrt{6}}{\alpha} \sqrt{\frac{\log d}{n}}. \quad (\text{A.21})$$

Unlike $\hat{\tau}_{jk}$ which is an unbiased estimator of τ_{jk} , $\hat{\rho}_{jk}$ is a biased estimator. To prove the desired result, we apply the following bias equation from Zimmerman et al. (2003):

$$\mathbb{E}\hat{\rho}_{jk} = \frac{6}{\pi(n+1)} \left[\arcsin(\Sigma_{jk}^0) + (n-2) \arcsin\left(\frac{\Sigma_{jk}^0}{2}\right) \right]. \quad (\text{A.22})$$

Equivalently, we can write

$$\Sigma_{jk}^0 = 2 \cdot \sin \left(\frac{\pi}{6} \mathbb{E}\hat{\rho}_{jk} + a_{jk} \right), \quad (\text{A.23})$$

where $a_{jk} = \frac{\pi \mathbb{E} \hat{\rho}_{jk} - 2 \cdot \arcsin(\Sigma_{jk}^0)}{2(n-2)}$. It is easy to see that $|a_{jk}| \leq \frac{\pi}{n-2}$. Therefore, for all $n > \frac{6\pi}{t} + 2$ (which implies that $|a_{jk}| \leq \frac{t}{6}$),

$$\mathbb{P} \left(\sup_{jk} \left| \hat{S}_{jk}^\rho - \Sigma_{jk}^0 \right| > t \right) \quad (\text{A.24})$$

$$= d^2 \mathbb{P} \left(\left| 2 \sin \left(\frac{\pi}{6} \hat{\rho}_{jk} \right) - 2 \sin \left(\frac{\pi}{6} \mathbb{E} \hat{\rho}_{jk} + a_{jk} \right) \right| > t \right) \quad (\text{A.25})$$

$$\leq d^2 \mathbb{P} \left(\left| \hat{\rho}_{jk} - \mathbb{E} \hat{\rho}_{jk} - \frac{6}{\pi} a_{jk} \right| > \frac{3}{\pi} t \right) \quad (\text{A.26})$$

$$\leq d^2 \mathbb{P} \left(\left| \hat{\rho}_{jk} - \mathbb{E} \hat{\rho}_{jk} \right| > \frac{3}{\pi} t - \left| \frac{6}{\pi} a_{jk} \right| \right) \quad (\text{A.27})$$

$$= d^2 \mathbb{P} \left(\left| \hat{\rho}_{jk} - \mathbb{E} \hat{\rho}_{jk} \right| > \frac{2}{\pi} t \right). \quad (\text{A.28})$$

Thus we get the desired result. \square

Appendix B: Other Proofs

In this Section, we prove the Theorem 3.1.

B.1. Some Useful Lemmas

Let $\Phi(\cdot)$ and $\phi(\cdot)$ be the cumulative distribution function and density function of standard Gaussian. We start with some preliminary lemmas on the almost sure limit of the Gaussian maxima and the standardized empirical processes.

Since $g_j = f_j^{-1}$ and $f_j(t) = \Phi^{-1}(F_j(t))$, we have $g_j(u) = F_j^{-1}(\Phi(u))$.

Lemma B.1. (Pickands (1963)) *If z^1, \dots, z^n are i.i.d. standard Gaussian random variables, then*

$$\mathbb{P} \left(\liminf_{n \rightarrow \infty} \frac{\sup_{1 \leq i \leq n} z^i - \sqrt{2 \log n}}{\log \log n / \sqrt{2 \log n}} = -\frac{1}{2}, \limsup_{n \rightarrow \infty} \frac{\sup_{1 \leq i \leq n} z^i - \sqrt{2 \log n}}{\log \log n / \sqrt{2 \log n}} = \frac{1}{2} \right) = 1. \quad (\text{B.1})$$

This Lemma implies that, for any $c > 0$, for large enough n , the standard Gaussian random variables z^1, \dots, z^n satisfy

$$\sup_{1 \leq i \leq n} z^i \in \left[\sqrt{2 \log n} - \left(\frac{1}{2} + c \right) \frac{\log \log n}{\sqrt{2 \log n}}, \sqrt{2 \log n} + \left(\frac{1}{2} + c \right) \frac{\log \log n}{2 \sqrt{\log n}} \right] \text{ almost surely.}$$

In the following, we set $c = \frac{1}{2}$. Then

$$\sup_{1 \leq i \leq n} z^i \in \left[\sqrt{2 \log n} - \frac{\log \log n}{\sqrt{2 \log n}}, \sqrt{2 \log n} + \frac{\log \log n}{\sqrt{2 \log n}} \right] \text{ for large enough } n \text{ a.s..}$$

Lemma B.2. (*Almost Sure Limit of the Standardized Empirical Process*) Consider a sequence of sub-intervals $[L_n^{(j)}, U_n^{(j)}]$ with both $L_n^{(j)} = g_j(\sqrt{\alpha \log n}) \uparrow \infty$ and $U_n^{(j)} = g_j(\sqrt{\beta \log n}) \uparrow \infty$, then for $0 < \alpha < \beta < 2$

$$\limsup_{n \rightarrow \infty} \sqrt{\frac{n}{2 \log \log n}} \sup_{L_n^{(j)} < t < U_n^{(j)}} \left| \frac{\tilde{F}_j(t) - F_j(t)}{\sqrt{F_j(t)(1 - F_j(t))}} \right| = C \text{ a.s.}$$

where $0 < C < 1$ is a constant.

The following lemma characterizes the behavior of a random sequence using a deterministic one.

Lemma B.3. For and $0 < \alpha < 2$, we have

$$\limsup_{n \rightarrow \infty} \frac{(\Phi^{-1})'(\max\{\tilde{F}_j(g_j(\sqrt{\alpha \log n})), F_j(g_j(\sqrt{\alpha \log n}))\})}{(\Phi^{-1})'(F_j(g_j(\sqrt{\alpha \log n})))} \leq C \text{ a.s.}$$

where $C > 0$ is some constant.

Proof. We only need to consider the case $\tilde{F}_j > F_j$.

First, for large enough n

$$\sqrt{\frac{\phi(\sqrt{\alpha \log n})}{\sqrt{\alpha \log n}}} \leq \phi \left(\sqrt{\alpha \log n} + \sqrt{\frac{2 \log \log n}{n^{1-\alpha/2}}} \right) \cdot n^{\alpha/4}. \quad (\text{B.2})$$

This is true since

$$\begin{aligned} & \phi \left(\sqrt{\alpha \log n} + \sqrt{\frac{2 \log \log n}{n^{1-\alpha/2}}} \right) \\ &= \frac{1}{\sqrt{2\pi}} \exp \left(-\frac{\alpha \log n}{2} - \frac{\log \log n}{n^{2-\alpha}} - \sqrt{\frac{2\alpha(\log n)(\log \log n)}{n^{1-\alpha/2}}} \right) \\ &= \phi(\sqrt{\alpha \log n}) \cdot R_n \end{aligned}$$

where $R_n = 1 - o(1)$.

Therefore,

$$\phi \left(\sqrt{\alpha \log n} + \sqrt{\frac{2 \log \log n}{n^{1-\alpha/2}}} \right) \cdot n^{\alpha/4} \geq \frac{n^{-\alpha/4}}{2\sqrt{\pi}}. \quad (\text{B.3})$$

Also,

$$\sqrt{\frac{\phi(\sqrt{\alpha \log n})}{\sqrt{\alpha \log n}}} = \frac{n^{-\alpha/4}}{(2\pi\alpha \log n)^{1/4}}. \quad (\text{B.4})$$

Thus, equation (B.2) follows from equations (B.3) and (B.4).

Further, using the fact that

$$1 - \Phi(t) \leq \frac{\phi(t)}{t} \quad \text{if } t \geq 1,$$

we have

$$\begin{aligned} \sqrt{\frac{2 \log \log n}{n}} \sqrt{1 - \Phi(\sqrt{\alpha \log n})} &\leq \sqrt{\frac{2 \log \log n}{n}} \sqrt{\frac{\phi(\sqrt{\alpha \log n})}{\sqrt{\alpha \log n}}} \\ &\leq \phi \left(\sqrt{\alpha \log n} + \sqrt{\frac{2 \log \log n}{n^{1-\alpha/2}}} \right) \sqrt{\frac{2 \log \log n}{n^{1-\alpha/2}}} \\ &\leq \Phi \left(\sqrt{\alpha \log n} + \sqrt{\frac{2 \log \log n}{n^{1-\alpha/2}}} \right) - \Phi(\sqrt{\alpha \log n}), \end{aligned}$$

where the last step follows from the mean value theorem.

Thus

$$\Phi(\sqrt{\alpha \log n}) + \sqrt{\frac{2 \log \log n}{n}} \sqrt{1 - \Phi(\sqrt{\alpha \log n})} \leq \Phi \left(\sqrt{\alpha \log n} + \sqrt{\frac{2 \log \log n}{n^{1-\alpha/2}}} \right).$$

Since Φ is a monotone function,

$$\Phi^{-1} \left(\Phi(\sqrt{\alpha \log n}) + \sqrt{\frac{2 \log \log n}{n}} \sqrt{1 - \Phi(\sqrt{\alpha \log n})} \right) \leq \sqrt{\alpha \log n} + \sqrt{\frac{2 \log \log n}{n^{1-\alpha/2}}}.$$

Using the fact that

$$F_j(g_j(t)) = \Phi(t),$$

we have

$$\begin{aligned} \Phi^{-1} \left(F_j \left(g_j(\sqrt{\alpha \log n}) \right) + \sqrt{\frac{2 \log \log n}{n}} \sqrt{1 - F_j \left(g_j(\sqrt{\alpha \log n}) \right)} \right) \\ \leq \sqrt{\alpha \log n} + \sqrt{\frac{2 \log \log n}{n^{1-\alpha/2}}}. \end{aligned}$$

From Lemma B.2, for large enough n ,

$$\tilde{F}_j(t) \leq F_j(t) + \sqrt{\frac{2 \log \log n}{n}} \cdot \sqrt{1 - F_j(t)}.$$

Therefore

$$\Phi^{-1} \left(\tilde{F}_j \left(g_j(\sqrt{\alpha \log n}) \right) \right) \leq \sqrt{\alpha \log n} + \sqrt{\frac{2 \log \log n}{n^{1-\alpha/2}}}.$$

Finally, we have that

$$\begin{aligned} (\Phi^{-1})' \left(\tilde{F}_j \left(g_j(\sqrt{\alpha \log n}) \right) \right) &= \frac{1}{\phi \left(\Phi^{-1} \left(\tilde{F}_j \left(g_j(\sqrt{\alpha \log n}) \right) \right) \right)} \\ &\leq \sqrt{2\pi} \exp \left(\frac{\left(\sqrt{\alpha \log n} + \sqrt{\frac{2 \log \log n}{n^{1-\alpha/2}}} \right)^2}{2} \right) \\ &= O \left(n^{\alpha/2} \right) \\ &\asymp (\Phi^{-1})' \left(F_j \left(g_j(\sqrt{\alpha \log n}) \right) \right). \end{aligned}$$

This finishes the proof. □

For any $\gamma > 0$, we define the following sub-intervals.

$$I_{1n} := \left[g_j(0), g_j \left(\sqrt{\alpha \log n} \right) \right] \quad I_{2n} := \left[g_j \left(\sqrt{\alpha \log n} \right), g_j \left(\sqrt{\beta \log n} \right) \right]$$

and

$$I_{3n} := \left[g_j \left(\sqrt{\beta \log n} \right), g_j \left(\sqrt{\left(\frac{7}{4} - \gamma \right) \log n} \right) \right].$$

with $0 < \alpha < 1 < \beta < 2$.

In the following, we define

$$\begin{aligned} u_n^* &:= \sqrt{2 \log n} - \frac{\log \log n}{\sqrt{2 \log n}} \\ t_n^* &:= \sqrt{2 \log n} + \frac{\log \log n}{\sqrt{2 \log n}}. \end{aligned}$$

Lemma B.4. *For all $t \in I_{1n} \cup I_{2n} \cup I_{3n}$, we have*

$$\mathbb{P} \left(\frac{1}{n} \leq \tilde{F}_j(t) \leq 1 - \frac{1}{n} \text{ for large enough } n \right) = 1.$$

Proof. From Equation (B.1), we have

$$\mathbb{P} \left(\sup_{1 \leq i \leq n} z_i \in \left[\sqrt{2 \log n} - \frac{\log \log n}{\sqrt{2 \log n}}, \sqrt{2 \log n} + \frac{\log \log n}{\sqrt{2 \log n}} \right] \text{ for large enough } n \right) = 1.$$

From the previously described transformation scheme, this implies that

$$\mathbb{P} \left(\sup_{1 \leq i \leq n} x_j^i \in [g_j(u_n^*), g_j(t_n^*)] \text{ for large enough } n \right) = 1.$$

Therefore

$$\mathbb{P} \left(\sup_{1 \leq i \leq n} x_j^i \notin I_{1n} \cup I_{2n} \cup I_{3n} \text{ for large enough } n \right) = 1.$$

From the definition of \tilde{F}_j , only the values greater or equal to the $\sup_{1 \leq i \leq n} x_j^i$ are truncated. The result then follows. \square

B.2. Proof of Theorem 3.1

Proof. of Theorem 3.1.

Due to symmetricity, we only need to conduct analysis on a sub-interval of $I_n^s \subset I_n$:

$$I_n^s := \left[g_j(0), g_j \left(\sqrt{\left(\frac{7}{4} - \gamma \right) \log n} \right) \right].$$

Recall that For any $\gamma > 0$, we define

$$I_{1n} := \left[g_j(0), g_j \left(\sqrt{\alpha \log n} \right) \right] \quad I_{2n} := \left[g_j \left(\sqrt{\alpha \log n} \right), g_j \left(\sqrt{\beta \log n} \right) \right]$$

and

$$I_{3n} := \left[g_j \left(\sqrt{\beta \log n} \right), g_j \left(\sqrt{\left(\frac{7}{4} - \gamma \right) \log n} \right) \right].$$

with $0 < \alpha < 1 < \beta < 2$.

By Lemma B.4, we know that on $I_{1n} \cup I_{2n} \cup I_{3n}$, $\frac{1}{n} \leq \tilde{F}_j(t) \leq 1 - \frac{1}{n}$ for large enough n almost surely. Therefore, we only need to analyze the term

$$\sup_{t \in I_{1n} \cup I_{2n} \cup I_{3n}} \left| \Phi^{-1} \left(\tilde{F}_j(t) \right) - \Phi^{-1} (F_j(t)) \right|.$$

First, we consider the term

$$\sup_{t \in I_{1n}} \left| \Phi^{-1} \left(\tilde{F}_j(t) \right) - \Phi^{-1} (F_j(t)) \right|.$$

Since Φ^{-1} is continuous on $\left[\min\{\tilde{F}_j(g_j(0)), F_j(g_j(0))\}, \max\{\tilde{F}_j(g_j(\sqrt{\alpha \log n})), F_j(g_j(\sqrt{\alpha \log n}))\} \right]$ and is differentiable on the corresponding open set, by the mean-value theorem, for some ξ_n , such that

$$\xi_n \in \left[\min\{\tilde{F}_j(g_j(0)), F_j(g_j(0))\}, \max\{\tilde{F}_j(g_j(\sqrt{\alpha \log n})), F_j(g_j(\sqrt{\alpha \log n}))\} \right],$$

we have

$$\sup_{t \in I_{1n}} \left| \Phi^{-1} \left(\tilde{F}_j(t) \right) - \Phi^{-1} (F_j(t)) \right| = \sup_{t \in I_{1n}} \left| (\Phi^{-1})'(\xi_n) \left(\tilde{F}_j(t) - F_j(t) \right) \right|.$$

By Lemma B.3,

$$\begin{aligned} (\Phi^{-1})'(\xi_n) &\leq (\Phi^{-1})' \left(\max \{ F_j \left(g_j \left(\sqrt{\alpha \log n} \right) \right), \tilde{F}_j \left(g_j \left(\sqrt{\alpha \log n} \right) \right) \} \right) \\ &\leq C (\Phi^{-1})' \left(F_j \left(g_j \left(\sqrt{\alpha \log n} \right) \right) \right) = \frac{C}{\phi \left(\sqrt{\alpha \log n} \right)} \leq c_1 n^{\alpha/2} \end{aligned}$$

where C and c_1 are some generic constants. Using the Dvoretzky-Kiefer-Wolfowitz inequality, we have

$$\sup_{t \in I_{1n}} \left| \Phi^{-1} \left(\tilde{F}_j(t) \right) - \Phi^{-1} (F_j(t)) \right| = O_P \left(\sqrt{\frac{\log \log n}{n^{1-\alpha}}} \right).$$

Next, we consider the term

$$\sup_{t \in I_{2n}} \left| \Phi^{-1} \left(\tilde{F}_j(t) \right) - \Phi^{-1} (F_j(t)) \right|.$$

Since $\tilde{F}_j(t)$ approximates $F_j(t)$ in a faster rate on I_{2n}

$$\begin{aligned} \sup_{t \in I_{2n}} \left| \tilde{F}_j(t) - F_j(t) \right| &= O_P \left(\sqrt{\frac{2 \log \log n}{n}} \cdot \sqrt{1 - F_j \left(g_j \left(\sqrt{\alpha \log n} \right) \right)} \right) \\ &= O_P \left(\sqrt{\frac{2 \log \log n}{n}} \cdot \sqrt{\frac{n^{-\alpha/2}}{\sqrt{\alpha \log n}}} \right) \\ &= O_P \left(\sqrt{\frac{2 \log \log n}{n^{\alpha/2+1}}} \right). \end{aligned}$$

We have

$$\sup_{t \in I_{2n}} \left| \Phi^{-1} \left(\tilde{F}_j(t) \right) - \Phi^{-1} (F_j(t)) \right| = O_P \left(\sqrt{\frac{\log \log n}{n^{1+\alpha/2-\beta}}} \right).$$

Similarly, we have

$$\sup_{t \in I_{3n}} \left| \Phi^{-1} \left(\tilde{F}_j(t) \right) - \Phi^{-1} (F_j(t)) \right| = O_P \left(\sqrt{\frac{\log \log n}{n^{\beta/2-3/4+\gamma}}} \right).$$

From above, we choose

$$\beta = \frac{3}{2} - \gamma \quad \alpha = 1 - \gamma,$$

all terms vanish. Thus we get the desired result. \square

References

- BANERJEE, O., GHAOUI, L. E. and D'ASPREMONT, A. (2008). Model selection through sparse maximum likelihood estimation. *Journal of Machine Learning Research* **9** 485–516.
- CAI, T., LIU, W. and LUO, X. (2011). A constrained l1 minimization approach to sparse precision matrix estimation. *Journal of the American Statistical Association* **106** 594–607.
- CHEN, S. S., DONOHO, D. L. and SAUNDERS, M. A. (1998). Atomic decomposition by basis pursuit. *SIAM Journal on Scientific and Statistical Computing* **20** 33–61.
- CHRISTENSEN, D. (2005). Fast algorithms for the calculation of Kendall's τ . *Computational Statistics* **20** 51–62.
- DEMPSTER, A. P. (1972). Covariance selection. *Biometrics* **28** 157–175.
- DRTON, M. and PERLMAN, M. D. (2007). Multiple testing and error control in Gaussian graphical model selection. *Statistical Science* **22** 430–449.
- DRTON, M. and PERLMAN, M. D. (2008). A SINful approach to Gaussian graphical model selection. *Journal of Statistical Planning and Inference* **138** 1179–1200.
- EDWARDS, D. (1995). *Introduction to graphical modelling*. Springer-Verlag Inc.
- FANG, H.-B., FANG, K.-T. and KOTZ, S. (2002). The meta-elliptical distributions with given marginals. *Journal of Multivariate Analysis* **82** 1–16.
- FRIEDMAN, J. H., HASTIE, T. and TIBSHIRANI, R. (2008). Sparse inverse covariance estimation with the graphical lasso. *Biostatistics* **9** 432–441.
- HOEFFDING, W. (1948). A Class of Statistics with Asymptotically Normal Distribution. *The Annals of Mathematical Statistics* **19** 293–325.
- HOEFFDING, W. (1963). Probability Inequalities for Sums of Bounded Random Variables. *Journal of the American Statistical Association* **58** 13–30.
- JAMES, G. M., RADCHENKO, P. and LV, J. (2009). Dasso: connections between the dantzig selector and lasso. *Journal Of The Royal Statistical Society Series B* **71** 127–142.
- KLAASSEN, C. A. J. and WELLNER, J. A. (1997). Efficient estimation in the bivariate normal copula model: Normal margins are least-favorable. *Bernoulli* **3** 55–77.
- KRUSKAL, W. H. (1958). Ordinal Measures of Association. *Journal of the American Statistical Association* **53** No. **284**. 814–861.
- LAM, C. and FAN, J. (2009). Sparsistency and rates of convergence in large covariance matrix estimation. *Annals of Statistics* **37** 42–54.
- LEEK, J. T. and STOREY, J. D. (2007). Capturing heterogeneity in gene expression studies by surrogate variable analysis. *PLoS Genet* **3** e161.
- LIU, H., LAFFERTY, J. and WASSERMAN, L. (2009). The nonparanormal: Semiparametric estimation of high dimensional undirected graphs. *Journal of Machine Learning Research* **10** 2295–2328.
- LIU, H., ROEDER, K. and WASSERMAN, L. (2010). Stability approach to regularization selection (stars) for high dimensional graphical models. In *Proceedings of the Twenty-Third Annual Conference on Neural Information Processing Systems (NIPS)*.

- MEINSHAUSEN, N. and BÜHLMANN, P. (2006). High dimensional graphs and variable selection with the lasso. *Annals of Statistics* **34**(3).
- PENG, J., WANG, P., ZHOU, N. and ZHU, J. (2009). Partial correlation estimation by joint sparse regression models. *Journal of the American Statistical Association* **104** 735–746.
- PICKANDS, J. (1963). Asymptotic properties of the maximum in a stationary gaussian process. *Transactions of the American Mathematical Society* **145** 75–86.
- RAVIKUMAR, P., WAINWRIGHT, M., RASKUTTI, G. and YU, B. (2009). Model selection in Gaussian graphical models: High-dimensional consistency of ℓ_1 -regularized MLE. In *Advances in Neural Information Processing Systems 22*. MIT Press, Cambridge, MA.
- RAVIKUMAR, P., WAINWRIGHT, M. J. and LAFFERTY, J. (2010). High-dimensional l1 model selection using l1-regularized logistic regression. *Annals of Statistics* **38** 1287–1319.
- ROTHMAN, A. J., BICKEL, P. J., LEVINA, E. and ZHU, J. (2008). Sparse permutation invariant covariance estimation. *Electronic Journal of Statistics* **2** 494–515.
- TIBSHIRANI, R. (1996). Regression shrinkage and selection via the lasso. *Journal of the Royal Statistical Society, Series B, Methodological* **58** 267–288.
- TSUKAHARA, H. (2005). Semiparametric estimation in copula models. *Canadian Journal of Statistics* **33** 357–375.
- YUAN, M. (2010). High dimensional inverse covariance matrix estimation via linear programming. *Journal of Machine Learning Research* **11** 2261–2286.
- YUAN, M. and LIN, Y. (2007). Model selection and estimation in the Gaussian graphical model. *Biometrika* **94** 19–35.
- ZIMMERMAN, D. W., ZUMBO, B. D. and WILLIAMS, R. H. (2003). Bias in estimation and hypothesis testing of correlation. *Transformation* **24** 133–158.